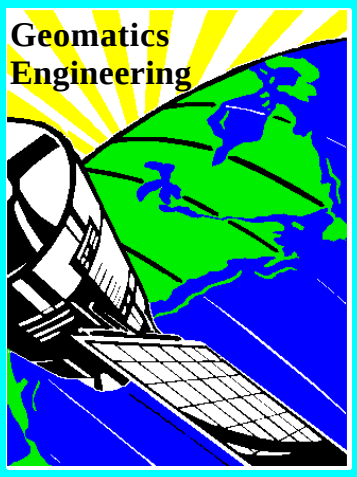

UCGE Reports
Number 20072

Department of Geomatics Engineering

GPS Integrated Systems For Precision Farming

By
Hazen L. Gehue

December 1994

Calgary, Alberta, Canada

THE UNIVERSITY OF CALGARY

GPS Integrated Systems for Precision Farming

by

Hazen L. Gehue

A THESIS

SUBMITTED TO THE FACULTY OF GRADUATE STUDIES

IN PARTIAL FULFILLMENT OF THE REQUIREMENTS FOR THE

DEGREE OF MASTER OF SCIENCE

GEOMATICS ENGINEERING

CALGARY, ALBERTA

DECEMBER, 1994

ABSTRACT

The consequences of homogeneous treatments of agricultural fields is investigated and quantified for several farm scale test sites throughout Alberta. A series of integrated data collection systems using GPS to locate and map information such as salinity and yield are discussed in stages of design, software, hardware and implementation. Results from the spatial data analysis produced a prescription map describing the fertilizer inputs for specified regions of the field. To fulfill the variable input requirements, a real time differential GPS system integrated with a variable rate air seeder was designed and implemented at each of the test sites.

The theory and performance of the GPS equipment and techniques used to verify the accuracy and repeatability of
the derived positions are discussed and results from analysis software developed are presented.

ACKNOWLEDGMENTS

This thesis is dedicated entirely to my wife Georgette and my two children Carleen and Christopher. Their support and encouragement kept my motivation and spirits high.

Special thanks are extended to my supervisor Dr. M. Elizabeth Cannon as well Tom Goddard and Colin McKenzie for their time, technical support, advice and proof reading in putting together this thesis.

The Precision Farming Project was made possible through the substantial efforts of the research team. Thank you to Murray Green, Doug Penney, Marshall Eliason, Dan Heaney, Sheilah Nolan, Germar Lohstraeter, Karen Skarberg and Neil Clark from Alberta Agriculture.

Appreciation is extended to Dr. M. E. Cannon and Dr. G. Lachapelle for allowing me to use this project for

my thesis research during my term as a research associate.

TABLE OF CONTENTS

LIST OF TABLES

TABLE

LIST OF FIGURES

FIGURE

CHAPTER 1

INTRODUCTION

It has long been accepted by agricultural producers that homogenous treatment of fields reflects in sub-optimal crop production due to the variability of many factors within the field (Schueller, 1992). If the producer could be furnished with detailed, accurate and repeatable maps describing these variabilities and if relationships among the numerous causes of variation could be determined, then a very powerful farm management tool can been derived (Bethham, 1994). This would enable the producer to make informed decisions regarding land use to optimize crop production on a sub field basis to yield a more sustainable and economical farming practice.

Much of the agronomic research work to date has been performed on small scale plots (e.g., Robertson et al., 1994; Nyborg et al., 1993). The research has been successful but it has not been typical at the farm scale due to the sometimes drastic changes in landscape features, inherent variabilities in the soil, ground water and migration tendencies of

nutrients and salinity. In the past it has been very difficult to attain the vast amounts of data required for detailed maps depicting the field behaviour in crop response, salinity, soil variation and nutrient migration. Additionally, the lack of navigation capabilities to return and treat the field in an optimal manner, has been overcome with advances in computer technology, intelligent sensor hardware and the now operational Global Positioning System (GPS).

A joint project by The University of Calgary, Alberta Agriculture Food and Rural Development and The University of Alberta attempts to characterize these variabilities at the farm scale and create a management scheme for the regions that can be optimized. The data collection, integrated systems and navigation research form the basis of this thesis.

1.1 The Consequences of Ignoring Variability

A variety of different soils exist across any given field in the province of Alberta. Even the most subtle changes in elevation, aspect and parent material can produce different and changing soil characteristics, behaviour and response. This results in a range of potential growing conditions across the landscape (Goddard, 1994).

Historically, farm fields have been treated as homogeneous units. Cultivation occurred with the same depth and often at the same time of the year. Seeding was done with the same variety of wheat or forage mixture. Landscape features such as a hilltop knoll allowed soils to erode faster than soils in the lower depression regions. This creates differences not only in crop productivity but weed types and populations as well. Over time, the soil and therefore field conditions and yield responses begin to vary more dramatically.

The consequences of ignoring these variabilities are:

- A wide range in moisture conditions caused by soil texture, thickness, percolation and run off capabilities.
- A wide range of erosion / deposition conditions caused by mechanical forces of wind, water and farm machinery. Regions of high erosion will have characteristics resembling the subsoil rather than topsoil.
- A wide range in fertility caused by heterogeneous soils. The lower landscape regions can potentially have twice the organic matter content and nitrate levels as an upper region (Mann, 1994).
- A wide range of weed species and populations which exist according to the landscape element they are best suited. This makes the weed infested regions more difficult to control resulting in a mixture of weed and crop (dockage) at harvest time.

The above existing farm conditions will continue to impact the farm management and economics over the long term. Continuation of a constant agronomic practice on a heterogeneous field will further increase the range in soil types, growing conditions and pest problems. Several

strategies to slow or reverse the spiral tendencies can be attempted:

- Divide the field into smaller fields based on the soil and landscape characteristics.
- Adopt variable management and cultural schemes to the landscape.
- Conduct reclamation procedures to physically change or narrow the range of soil conditions within the field.

Some of the available practices to employ in the above strategies are:

- Identify the extremes in the field and perform detailed soil analysis to determine the scale of the variation. This allows the determination of the weighted averages of the field inputs and to apply variable rates of fertilizer or herbicide.
- Spot spray or fertilize regions of extreme weed infestation or nutrient deficiency. Two equipment passes may be required to fulfill this approach.

- Spread manure or old bales on regions of high erosion or sandy areas where organic return is minimal (Goddard, 1994).

The topic of this thesis is to develop integrated data collection systems to identify the extreme regions at four test sites within Alberta. Fields are evaluated based on yield response, degree of salinity, soil sampling results and variations in digital terrain modeling (DTM). All data is position tagged using **DGPS** based on the L1 C/A pseudorange code solution with applied smoothing. Additional information (nutrient analysis and field history) are collated to assist in the determination of the variable fertilizer prescription map.

The application of variable blends and bands of fertilizer is performed by locating regions defined by the prescription map in the field using real time differential **GPS** (RTDGPS) and activating the servo motor control on the air seeder to dispense the required fertilizer.

The **DGPS** and **RTDGPS** solutions use the narrow correlator technology (Van Dierendonck et al, 1992) in the NovAtel GPS receiver and surpassed the project minimum requirements in

root mean square (RMS) accuracies of 0.5 m horizontally and 1.0 m vertically both in post mission and real time. Position accuracies were verified by comparisons with a carrier phase “on the fly” (OTF) and repeatability analysis.

1.2 Thesis Outline

The precision farming initiative is a two phase approach for the first harvest to seeding season. Phase I is of data collection campaigns using a series of sensors integrated with **GPS**. Phase II is the use of **RTDGPS** to control a variable rate fertilizer applicator. Hardware used and software developed to build the integrated systems are described in Chapter 2. Of particular interest was the magnitude of the crop variation as well as salinity conditions, landscape features (for terrain modeling), location of calibration transects (i.e., square metre cuts, Time Domain Reflectrometry (TDR) probe points, soil moisture, ground truthing crop sampling) and locations of soil sample drill holes for soil mapping and nutrient determination.

Chapter 3 discusses the software developments and enhancements for the post processing and analysis in Phase I and II. The analysis of the GPS performance in terms of horizontal and vertical accuracies and the repeatability of heights over time were of interest. The methodology and implementation of the **RTDGPS** system working in conjunction with the prescription map is also discussed.

The test sites are described and the results of Phase I in terms of crop response and **DGPS** accuracies are discussed in Chapter 4.

Chapter 5 discusses the performance of the **RTDGPS** as compared to post mission results and high precision carrier phase **OTF** results. A slight degradation was experienced due to the effects of latency in the presence of Selective Availability (SA) but the project accuracies were still exceeded.

Chapter 6 contains the conclusions and recommendations based on the research in this thesis. Offshoot benefits to the project are optimization of the crop input/output

economics on a sub-field basis and more environmentally responsible farming practices.

CHAPTER 2

INTEGRATED GPS AND AGRICULTURE SENSORS

Position and navigation requirements for the precision farming project are being investigated by using the Global Positioning System (GPS) deployed and maintained by the United States Department of Defense. Two GPS receivers are used in differential mode (DGPS) either as a stand alone system to attain a 3-D position or integrated with external hardware sensors. The DGPS position is correlated with attribute information for input to a Geographical Information System (GIS).

2.1 GPS Receiver Component

The GPS receivers used in this project were the NovAtel 10 channel, single frequency, C/A code, GPSCARD™ that use the narrow correlator spacing technology to provide 10 cm pseudorange resolution (Fenton et al., 1991; Van Dierendonck et al., 1992). The GPSCARD™ model is directly mounted into an ISA slot (expansion bay) for direct docking capabilities to a

laptop computer. The NovAtel receivers used in differential mode, with the geodetic antenna (model 501) and accompanying chokerings, have achieved submetre accuracies in previous research projects when phase smoothing has been performed on the code (Cannon and Lachapelle, 1992a).

2.2 Computer Component

The computers (386 ***Compac***^{TM} and 386 ***Grid***^{TM}) used in Phase I were data loggers. Due to the mass of data collected a hard disk was required. Data collection was performed at a 1 Hz rate which translates into approximately 3 Megabytes of raw ASCII data per hour per GPS receiver. This coupled with long data collection campaigns and several sites to be done are an example of the volumes of data to be handled.

2.3 GPS Data Logging Software (*LOGNOVA1*)

Many of the data collection campaigns are not repeatable (e.g., yield data). To minimize the potential of data loss, custom logging software was developed to accommodate integrity and safety of the data as well as a few necessary options to allow time and attribute tagging.

2.3.1 Data Integrity and Safety

To ensure that the received data was valid, tests were performed on the incoming data string to verify correctness and quality. The primary cause of lost data is hardware failure (i.e., hard disk failure), sudden electrical surges or loss of power causing abnormal disk management. Since all of the programs are ***DOS***™ based, this creates an error in file closing. The data is lost and non recoverable. To prevent against this, data is buffered and saved every five minutes and file markers forced onto the hard disk. If power is interrupted only the buffered data is lost.

2.3.2 On-The-Fly Electronic Field Book

To be able to time and attribute tag positions, areas, profiles and trajectories of interests in any field, an electronic field book was developed to operate within the logging software ***LOGNOVA1***. The user activates the field book via a hot-key at the moment of interest. The GPS time is logged and the user could now enter pertinent site data while

maintaining logging. This attribute information will allow for the sorting of the position results for several different tasks such as:

- Determination of perimeters and areas of wetlands, non-harvested crop, non-cropped regions and physical obstructions on site (i.e., a windmill) for masking during surfacing.
- Determination of profiles along test transects and truthing lines.
- Determination of instant (one epoch) or mean positions (over several epochs) of points of interests (i.e., soil sample drill holes, square metre truthing samples, TDR probe points).

The data logging procedure was necessary to ensure that the information of interest was correctly located and easily extractable from the GPS position solution file.

2.4 Yield Monitor External Sensor

In order to determine the magnitude and spatial relationship of the field variability in crop response an external device that would measure instantaneous crop throughput was required. The Yield Monitor 2000 produced by Ag Leader Technology (Ames, Iowa) was used in this project.

2.4.1 Yield Monitor Features

The monitor is RS232 serial communication compatible at a fixed output rate of 1Hz. It is a compact, easily transportable and lightweight unit that can be set to communicate with any of the major combines that have been installed with the necessary sensors. The unit has the following capabilities (Yield Monitor 2000 User Manual, 1993):

- Measures and displays instantaneous yields (Bu per Ac), grain flow (Bu per Hr), combine (speed based on shaft rotation in MPH), harvesting rate (Ac/Hr).
- Calculates, displays and records average yield (Bu per Ac), area (Ac), distance (Ft or Mi), grain weight (Lb, wet grain

(Bu @ std %), dry grain (Bu @ std %), average field moisture(%), date and time load was started.

- Variable settings of field and load, row spaces and # rows, load moisture, grain type.

Each of the combines (John Deere 9600, Case IH 1680 and AgCo R-72) had to be custom fitted with the necessary sensors to collect the data required for the yield monitor to perform its calculations and displays. The combine sensors are fixed mounted and are not transportable to a different model or make of combine.

2.4.2 Yield Monitor Field Calibrations

Each combine must be calibrated for the sensor. This is performed by measuring out a fixed distance (200 ft is recommended) and driving the combine this distance. By comparing the distance calculated by the monitor one can make adjustments to the sensor. The test is performed until the measured distance is the same as the distance traveled calculated by the monitor. The only other field setting required is to determine physically when the monitor believes

that the header is up (not harvesting) or down (harvesting). This is set by the operator of the combine. The header is set to the desired height to indicate when harvesting has stopped. The monitor is then adjusted to reflect this condition. The end result is that when the header is up, the distance and area count cease to increment. This is important to know because the entire procedure of grain pickup to hopper has a delay which is reflected in the monitor readings (i.e., even though the header sensor indicates that no grain is being harvested the monitor indicates that there is still grain flow in the clean grain elevator).

2.4.3 Yield Monitor Output

The inner algorithms of the yield monitor are proprietary knowledge of Ag Leader Technology who developed the product. The following is a basic description of how the necessary information for the monitor is collected:

- The header sensor indicates “down” so crop is being taken up into the combine.

- The grain is separated and sent up the conveyor belt of the clean grain elevator at a measured speed and conveyor paddle volume.
- The grain is thrown against a sensor plate at the top of the clean grain elevator where the force of impact is measured.
- From the combine sensors ground speed pulses (accumulated during load), ground speed (MPH), elevator speed (RPM), Flow sensor force (Lb) and grain flow rate (Lb per Sec) are input to the yield monitor.

2.4.4 GPS - Yield Monitor Integration

To map out the degree of variability of any field, two quantities must be determined. First, what is the magnitude of the instantaneous crop response and secondly, where is it located in the field. The Ag Yield Monitor and DGPS solve these questions respectively. In order to correlate the two inputs, the systems were combined via software integration and physically connected via a RS232 communication cable. A standard serial communication library was added to ***LOGNOVA1*** to

produce ***AGYLD1***. The following flowchart (Figure 2.1) outlines the logic in the integrated system.

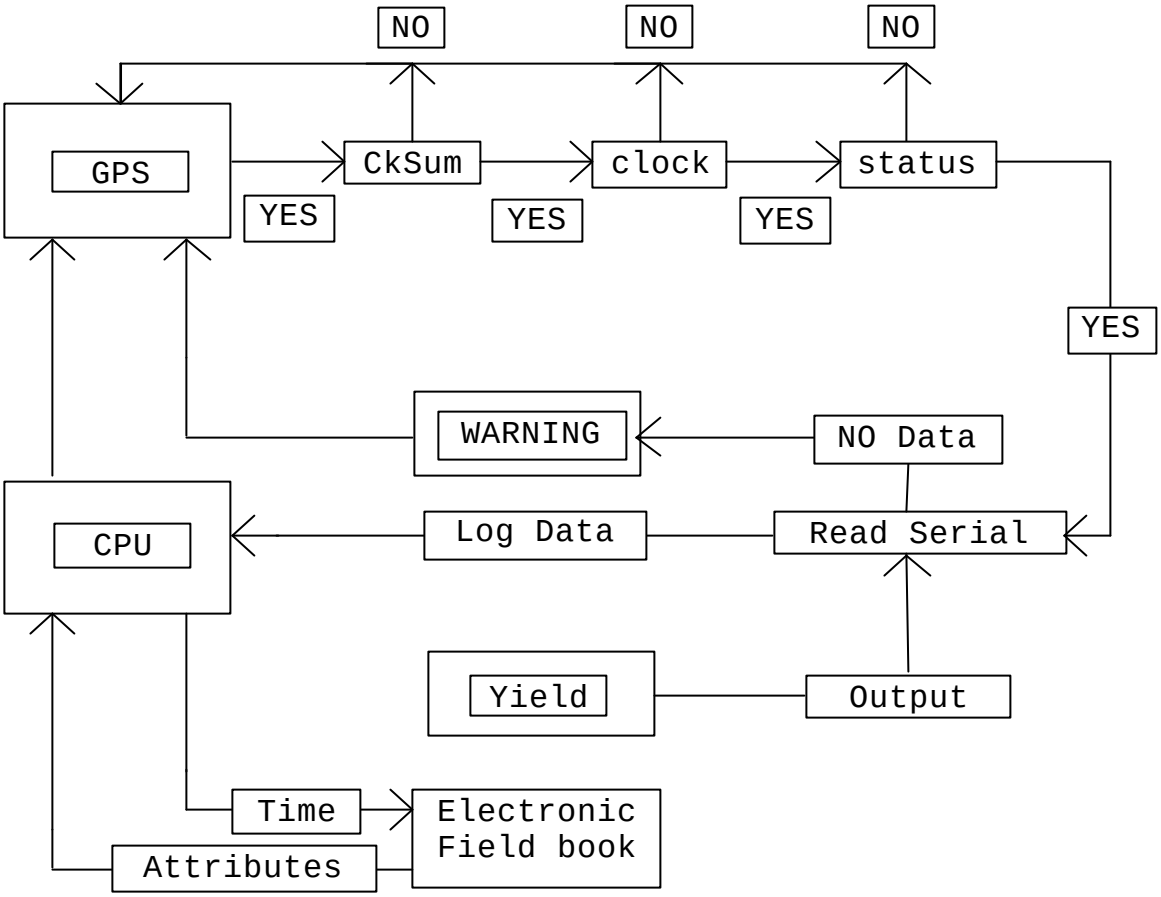

Figure 2.1 - Flow chart - GPS/Yield Monitor Integration

Once the GPS has passed a quality control algorithm, the serial port is polled for available data. If no data exists

then a warning message is set to the user to request a system check (i.e., check cable or power to yield monitor). The valid GPS data is logged regardless of the yield monitor response. If the serial port has registered an interrupt, the data is retrieved and time stamped with the GPS time and logged to a separate file. The data safety approach in ***AGYLD1*** is the same as was implemented in ***LOGNOVA1***.

2.5 EM38 Conductivity meter

The EM38 conductivity meter is an external sensor device that can indirectly measure the degree of salinity in the soil. Previous research in the field of salinity has show the EM38 to be repeatable to within 1.1 dSm^{-1} at common points (Lachapelle et al., 1992). If the location of potentially highly saline areas and migration tendencies can be mapped and modeled then this data can be correlated to yield in attempts to explain or predict crop response.

2.5.1 EM38 Conductivity Features

Several instruments have been introduced for determining the salinity in a field by measuring the apparent soil electrical conductivity (Wollenbaupt et al., 1986). The EM38

is an electromagnetic induction meter developed by Geonics of Canada. It provides salinity readings in the plant root zone by overcoming the limitations of soil-electrode contact (Rhoades and Corwin, 1981). The EM38 introduces very small “eddy currents” into the soil and measures the intensity of the primary and secondary magnetic fields created (Geonics Limited Technical Note TN-21). The EM38 used in this project has an analog output at 4Hz. It is RS232 serial communication compatible but the signal must be converted to digital in order to interface with a computer.

2.5.2 EM38 Field Calibrations

Before the EM38 can be used reliably it must undergo an initial inphase nulling before each survey. The inphase nulling is required for both the horizontal and vertical operating modes of the EM38. Calibration steps are outlined clearly in the user manual. An additional and ongoing calibration of the EM38 had to be performed due to the drift in the 8 byte A to D converter system. This was performed by stopping periodically and logging the reading from the EM38 display and the reading from the computer screen. The

digitally converted values should have been one quarter the EM38 analog values but this was not always the case. The calibrations were graphed after each session and a best fit drift scalar was determined to be used later in the salinity conversion calculations.

2.5.3 EM38 Output

The EM38 output value is recorded on channel one of the eight channel Maron A/D converter output and has to be converted back to EM38 standard readings (as if the measurement had been directly recorded from the EM38) using the best fit drift value as mentioned in Section 2.5.2. This value, coupled with the measured soil temperature, texture and moisture, can then be used to compute the salinity at any point (McKenzie et al., 1989). The collection of points can be transferred to a surfacing routine such as those found in ***Surfer***™ or ***GRASS***™ and a salinity map created.

2.5.4 GPS - EM38 Integration

The integration technique for the EM38 uses the same approach as the yield monitor. The integration engine was designed such that any serial peripheral that has a continuous output could be easily combined in software with the GPS receiver. Refer to Figure 2.1 in Section 2.4.4. By replacing the Yield Monitor sensor with the EM38 sensor in the integration scheme the ***AGSALT1*** data logger is created. The only difference to contend with is the 4 Hz output of the EM38. The most current record was logged and the others discarded because the GPS receiver was operating at 1 Hz.

2.6 Real Time DGPS Hardware

The computation requirements for Phase II were much more demanding than those in Phase I. The problem at hand was real-time navigation. The raw data extracted off the ***NovAtel GPSCard™*** now had to be used to compute corrections and transmit the information to the remote receiver. The increase in computational intensity resulted in an upgrade of computer equipment and the addition of a radio link for data transmission between the monitor and remote receivers.

2.6.1. DGPS Computer Hardware

Two rugedized 486 ***GRID***™ 1680 laptop computers operating at 25 MHz with 240 Megabytes of hard disk space were used for the real time component of the project. Additionally, two ***GRID***™ 1600 series expansion trays were required to house the ***NovAtel GPSCard***™ receivers and an additional serial communication card required to accommodate the second RS232 communications required for the system integration. The laptop computer interfaced with the expansion tray via a docking station to make a very compact and lightweight computer system.

2.6.2 DGPS Radio Link

A radio link was required to transmit in real time the differential corrections and correction rates to the remote receiver operating up to one kilometre away. Since the monitor to remote separation distances were short, the use of a low power, line of site radio system was selected. GRE America produces a radio suitable for this task.

The Global Integrated Network Access (***GINA***^{TM}) 6000 is a stand alone, high frequency radio transceiver that uses Spread Spectrum technology. It transmits data synchronously in the range of 902-928 MHz in speeds of 128 kilo bits per second (KBPS) in half duplex. It is RS232 serial communication compatible at data rates of 2400, 4800,9600 and 19,200 baud. The ***GINA***^{TM} will automatically resend information until it is received 100% correctly (GRE America, 1993).

It operates on one watt of power and comes with a 6 inch 1 dB gain antenna which has an expected range of 1 mile. To enhance the range, 5 dB antennas replaced the standard antennas.

The ***GINA***^{TM} is a point to point radio system. The radio modems can only communicate with one other ***GINA***^{TM} transceiver at a time. The communication sequence must be pre-programmed into the units and a communication connection must be made before transmission can begin (Figure 2.2). The communication sequence is defined by the unique identification number assigned to each unit.

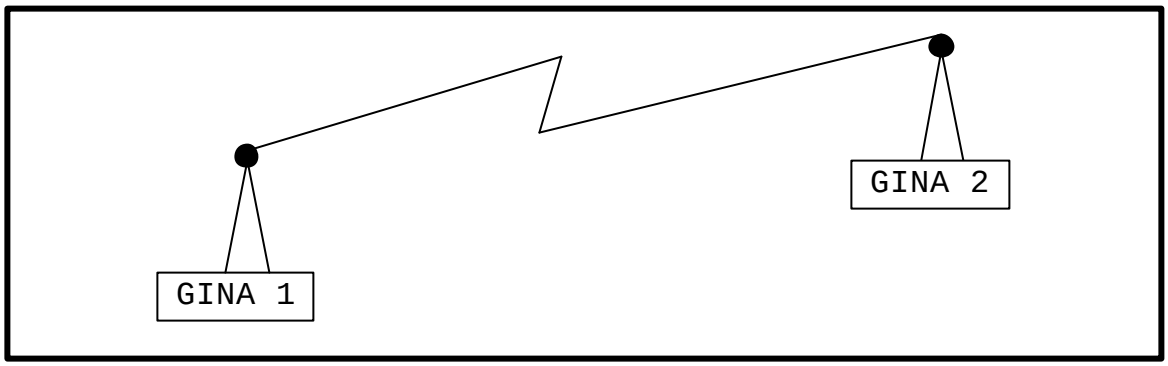

FIGURE 2.2 - *GINA*^{TM} **Radio Communication**

The radio modems can be linked in a daisy chain with all intermediate units acting as repeaters. This extends the range and transmits to regions not directly in line of sight as shown in Figure 2.3. The repeaters do not have to be fixed to any specific location and do not require a computer for

operation once the parameters have been set. This allows the repeaters to roam and to be placed temporarily at strategic locations. Radio shadowing can be avoided and continuous data reception achieved.

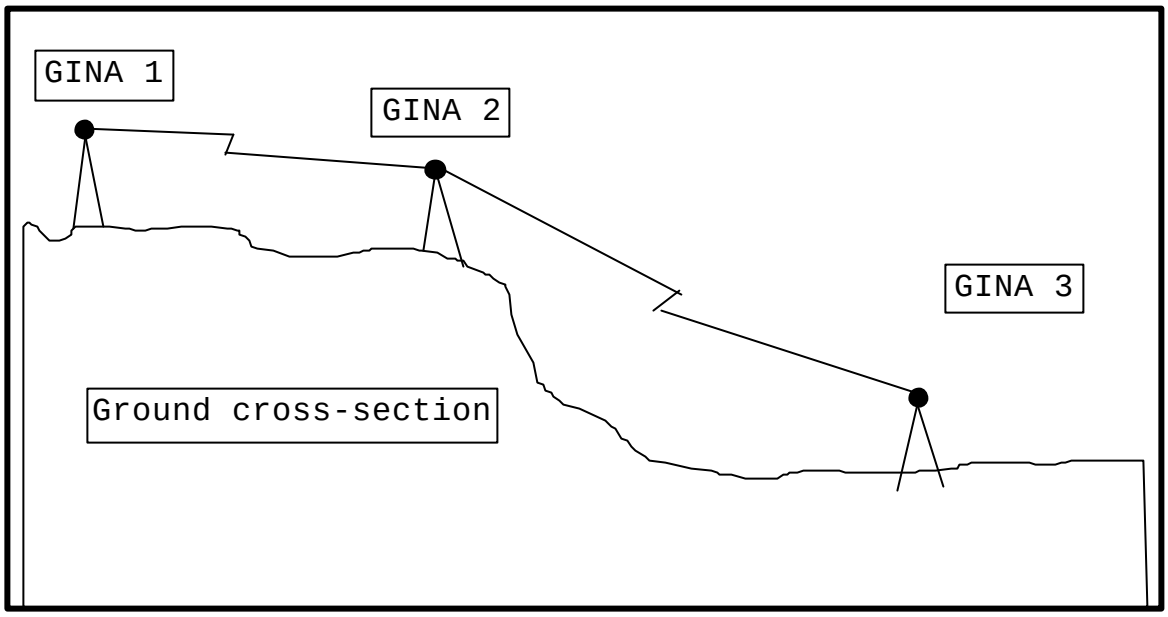

FIGURE 2.3 - GINA™ Daisy Chain

No official testing for the range of the radios was performed but with the improved 5 dB gain antenna the distance of 5 km point to point was routinely achieved.

Figure 2.4 illustrates the complete concept of the navigation system onboard the farm equipment. To attain economical and efficient use of this technology, the activities should be performed during normal farming operations as much as possible.

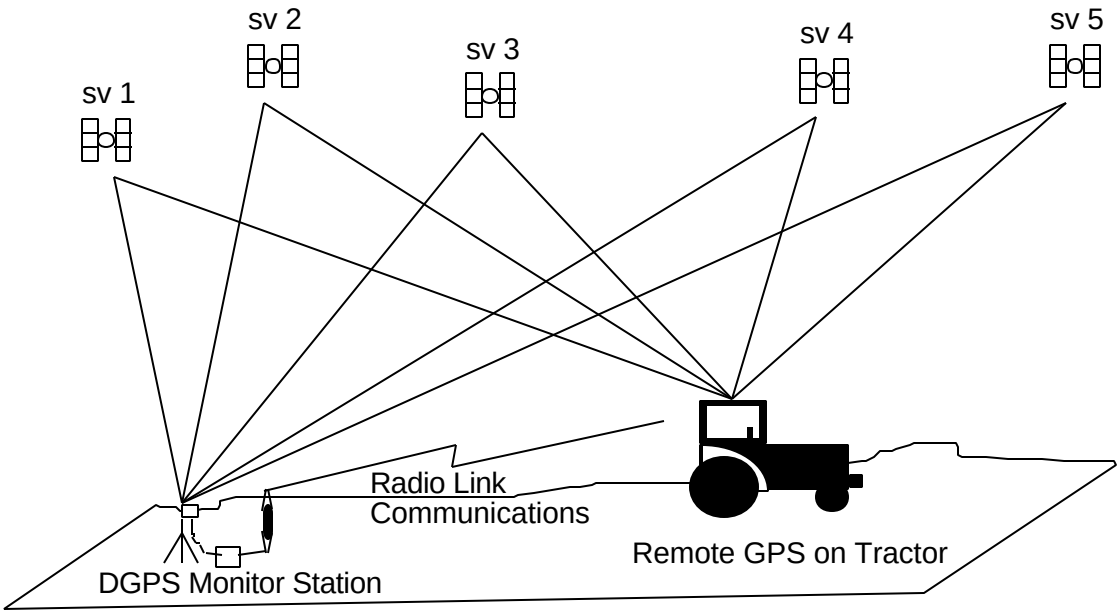

FIGURE 2.4 - Real Time DGPS Navigation

2.7 Variable Rate Controller

The final component for the integrated system is the variable rate controller. Its functions are to carry out the

instructions extracted from the prescription map. The hardware and software development of this system is provided by ***CONCORD***^{TM}, who holds a patent on variable rate technology (Anderson, 1994).

2.7.1 Motorola Microcontroller Unit

The system provided by ***CONCORD***^{TM} consists of the following components :

- Motorola M68HC11EVB Microcontroller Unit (MCU):

  Features: 8-bit, 2 MHz bus speed, on chip peripheral capabilities, DC frequencies, 8 Kbytes ROM, 512 bytes EPROM, 256 bytes RAM, WAIT and STOP modes for battery driven applications, RS232 serial communication compatible (Motorola, 1991)

- Two AcuPlant^{TM} digital to analogue converters for controlling the servo motors rotational speeds that regulated the independent flow of the fertilizer.

- Two bin air seeder for field treatment.

- Software for the communication of the above components and the algorithm to compute the desired bin output based on requested mass of field input and vehicle velocity.

2.7.2 MCU Communication

The MCU is an echo delay device which requires the inputs of two rotation periods, one for each motor, received via RS232 interface cable. A minimum delay of 50 ms is allowed between the transmission of each unsigned 2 byte character to allow the MCU to decode and echo back the value for verification. If the echo value does not match the transmitted value then re-transmission occurs until the export string is successfully received by the MCU.

Fixed to each servo motor is an analogue device that measures the motor’s shaft response and returns the measured period to the computer. This is very useful for monitoring the behaviour of the motors and provides instant detection of mechanical failure. If a time out delay of 500 ms occurs then the epoch is aborted and the next epoch handled. Shown below in Figure 2.5 is the in tow fertilizer air seeder and drill

rig. Mounted on the roof of the tractor is the GPS antenna and the 5 dB gain radio antenna. The computer, GPS receiver and radio modem are fixed mounted in the tractor’s cab. Power for the system is provided by the tractors electrical system.

Figure 2.5 - Variable Rate Farm Implement

Chapter 3

PROJECT SOFTWARE DEVELOPMENT

The research in this thesis was performed in two phases. Phase I consisted of the field data collection campaigns and post mission processing to identify the degree of variability within the field and the collection of additional information to assist in explaining the variability. Phase II is the real time implementation of the fertilizer blends and bands as dictated by the derived prescription map.

Approximately a Gigabyte of raw data was collected using the software developed for Phase I which utilized GPS (***LOGNOVA1***) and the GPS integrated systems (***AGYLD1, AGSALT1***). This amount of data requires automated processing in order to generate results in a reasonable time frame. Two programs had to be modified ***C3Navc***™, (Cannon, 1992) and **Flykin**™, (Lachapelle, 1992) for this purpose. Three programs had to be developed to manipulate the data for input to a GIS (***GPS_UTM1***, ***YLD_UTM1***, ***SALT_UTM1***).

Two additional programs were developed to determine the overall performance of the DGPS positions derived (***FLYVSC3N***) and a height repeatability study (***X_OVER1***) for verification of GPS heights in a single data session and inter-session.

Software for Phase II was developed to perform real time GPS navigation (***C3NavRT***™) integrated with a variable rate controller for fertilizer application.

3.1 Pseudorange Post Mission Software

C3Navc™ (***C***ombine ***C***ode ***C***arrier for GPS ***Nav***igation) is a post mission pseudorange GPS solution with the options to perform carrier phase smoothing on the pseudorange, height fixing and differential processing (herein refereed to as the ***SC*** solution). It is an ***IBM***™ ***DOS***™ platform ***FORTRAN***™ program converted to ***BorlandC***™ programming language (Cannon and Lachapelle, 1992). For all post mission processing carrier smoothing was used at both the monitor and remote station. If less than four satellites were tracked or the Geometric Dilution of Precision (GDOP) was greater than five then the height was held fixed at the input height (monitor station) or

at the mean of the last five heights (remote station). All remote position solutions have been differentially corrected.

The ***SC*** solution employs the following formulae for position determination in the above mentioned post processing scheme. The pseudorange observation equation is (Wells et al., 1989):

$$\mathbf{p} = r + \mathbf{d}r - \mathbf{c(dt-dT)} + \mathbf{d}_{ion} + \mathbf{d}_{trop} + e\mathbf{(p)} \quad \mathbf{(3.1)}$$

where **p** is the measure pseudorange, r is the computed geometric range ($\mathbf{||r - R||}$), **r** is the position vector of the satellite and **R** is the position vector of the receiver, $\mathbf{d}r$ is the error in the satellite orbit, **dt** and **dT** are satellite and receiver clock errors, $\mathbf{d}_{ion}$ and $\mathbf{d}_{trop}$ are the ionospheric and tropospheric delays and e is the measurement noise.

The carrier smoothing approach used is (Lachapelle et al., 1986):

$$Ps_k = W_1 P_k + W_2\{Ps_{k-1} + (F_k - F_{k-1})\} \qquad (3.2)$$

where Ps_k the smoothed measurement at epoch k_1 (m), P_k is the measured pseudorange at epoch k_1 (m), W_1 and W_2 are the sliding weight scalars and F_k, F_{k-1} are the measured carrier phase at the current epoch and previous epoch. The sliding weight scalars begin with a value of 1.0 for the pseudorange and 0.0 for the phase. As the epoch counter increases, the weights slide so that the emphasis is placed on the more accurate phase measurement. To counteract the effect of code carrier divergence due to the ionosphere, dual ramps operating in parallel are used (Cannon et al., 1993). The ramps are offset by half the selected ramp reset interval. Typically, this moving window technique reduces the time span that either ramp can be used and assumes a negligible difference in the code and carrier divergence exists during the number of epochs between resets.

The observation equation adjustment used is a least square adjustment model (Krakiwsky et al., 1987):

$$d = -(\mathbf{A}_t\ \mathbf{C}_l^{-1})^{-1}\ \mathbf{A}_t\ \mathbf{C}_l^{-1}\ \mathbf{w} \qquad (3.3)$$

where $d_{(nx1)}$ is the corrections to the approximate unknown parameters, **A** (mxn) is the measurement design matrix populated by the partial derivatives of Eqn. 3.1 , $\mathbf{C}_l$ (mxm) is the covariance matrix of the measurement noise. This matrix is evaluated by expressing the measurement resolution as a function of the pseudorange errors which vary with satellite elevation (Martin, 1980). **w** (mx1) is the misclosure vector, m is the number of measurements and n is the number of unknown parameters.

3.2 Carrier Phase Post Mission Software

Flykin^{TM} uses an On-The-Fly (OTF) ambiguity resolution technique (Lachapelle et al. 1992a) to resolve the double difference carrier phase ambiguities between a fixed monitor station and a remote receiver (herein refereed to as ***OTF*** phase solution). This high precision GPS kinematic approach has

achieved centimetre accuracy when the distance between the monitor and remote is less than 5 km (Lachapelle et al., 1993; Tiemeyer et al., 1994). It is an ***IBM^{TM} DOS^{TM}*** platform program written in ***BorlandC^{TM}*** programming language. The following phase and double difference phase formulation employed by the ***OTF*** phase solution are:

$$F = r + \mathbf{d}r + \mathbf{c(dt-dT)+N}l \mathbf{-d_{ion}+d_{trop}+}e\mathbf{(}F\mathbf{)} \qquad \mathbf{(3.4)}$$

$$D"F = D"r + D"\,\mathbf{d}r + D"\mathbf{N}l \mathbf{-}D"\mathbf{d_{ion}+}D"\mathbf{d_{trop}+}D"e\mathbf{(}F\mathbf{)} \quad \mathbf{(3.5)}$$

where F is the measure carrier phase , r is the computed geometric range (**||r - R||**), $\mathbf{d}r$ is the error in the satellite orbit, **dt** and **dT** are satellite and receiver clock errors, **N** is the integer cycle ambiguity, l is the carrier wavelength, $\mathbf{d_{ion}}$ and $\mathbf{d_{trop}}$ are the ionosphere and troposphere delays and e is the measurement noise.

$$D" = \mathbf{\{(*)_{sat2}-(*)_{sat1}\}_{Rx2} - \{(*)_{sat2}- (*)_{sat1}\}_{Rx1}} \qquad \mathbf{(3.6)}$$

The double difference indicator, D", is defined as the difference of observation equations (* , Eqn. 3.4) between satellites as depicted in Figure 3.1. The observations are extended to all satellites using a base satellite for all differencing. The choice of the base satellite is made automatically by the software although the option exists for user selection.

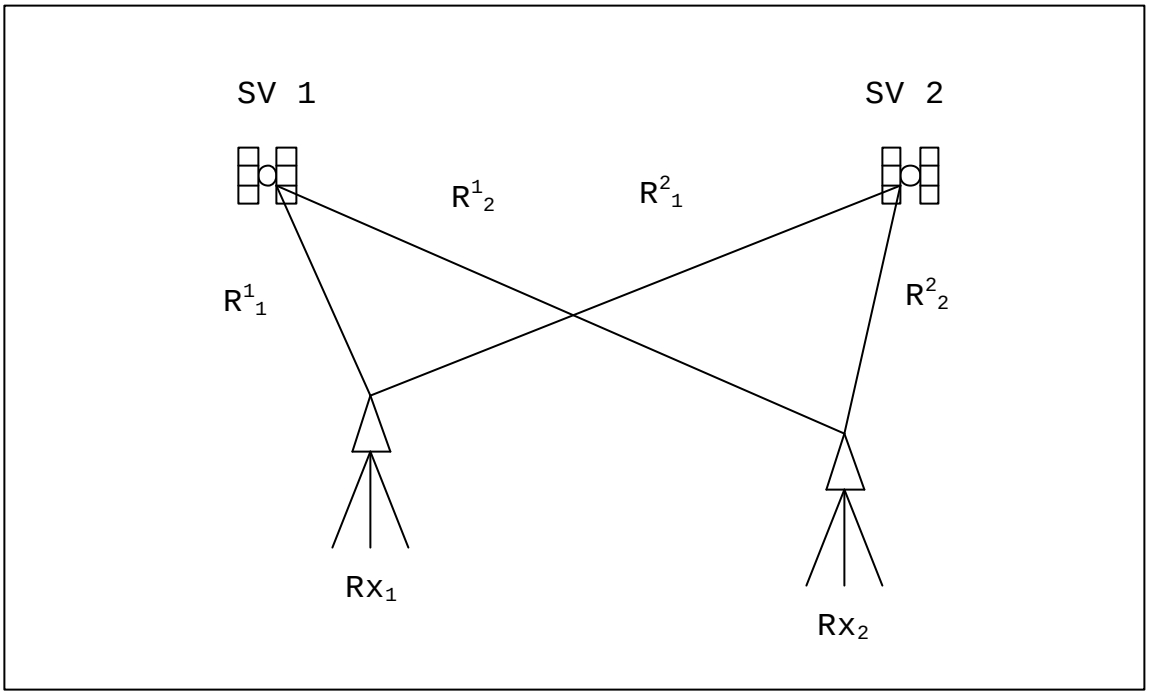

FIGURE 3.1 - Satellite - Receiver Double Difference

3.3 Modifications to C3Navc™ and Flykin™

Modifications were made to both programs to allow the following:

- Accept on the command line the option input file to allow ease of batch file capabilities.
- Accept the command line height of the antenna (HI) so all positions computed are reduced to ground. This would allow comparisons of heights over time, independent of the HI during the data collection period.
- Adjust the memory capabilities to house sufficient ephemeris records for long duration post processing.
- Add a data quality check (***C3Navc™*** only) to ensure that the range residuals were within a minimum tolerance. If the height was being fixed and a bad range was undetected then the subsequent epochs were effected causing severe position errors. When an unacceptable residual was detected the entire epoch was rejected.

3.4 Development of GPS_UTM1, YLD_UTM1, SALT_UTM1

It was decided by the precision farming panel to adopt a standard mapping procedure in which to base the GIS spatial relationships upon. The projection chosen was the Universal Transverse Mercator (UTM) NAD 83. A geographic to UTM grid coordinate conversion (T.J Blachut et al., 1979) was implemented and then modified to deal with the different integrated systems and logging procedures.

3.4.1 GPS_UTM1 Post Processing Software

The post mission software, ***GPS_UTM1***, was designed to operate with the data campaigns that used ***LOGNOVA1***. This was for stand alone GPS surveys (field perimeters, wetlands, profiles of truthing transects, DTM information etc.) and attribute determination (locations of soil samples, TDR probe points, square metre cuts etc.). Several different aspects of the data were required for different aspects of mapping.

Those involved with surfacing (DTM) required coordinates of the field perimeter and all of the three dimensional positions as well as the coordinates of features to be masked out. The soil scientist required only the positions of the

soil samples to combine with the soil analysis for mapping while the agronomists were interested in the profile information of the truthing transects and the location of the square metre cuts, for example. In order to be able to meet the requests of all of the parties, the sorting and formatting had to be based on the data collection period. The electronic field book was the link between the data collected and the position requirements of each party. ***GPS_UTM1*** was designed with the following options:

- doall: extract and convert all GPS geographic positions to UTM (i.e., DTM).
- parse: similar to ‘doall’ but the mean of “n” positions is extracted based on the parsing value (i.e., data thinning).
- event: search the message file (produced by the electronic field book) and extract the time and attribute information for each event logged.
- range: search the message file for two identical records, extract the times and messages. Compute the mean position of the attribute (i.e., soil sample location).

- traje: search for a “start” and “end” indicator in the message file. Extract out the corresponding positions between the times (i.e., perimeter of the field or profile).
- area: uses the same searching approach as ‘traje’ but also calculates the area (hectors and acres) of the closed trajectory (i.e., field acreage for harvest).

Based on the command line options inputted into the program, the GPS position as computed by the ***SC*** solution would be converted to the UTM mapping plane and attribute tagged with the corresponding message file information. ***GPS_UTM1*** will also work with the other login software but ignores the data collected via system integration.

3.4.2 YLD_UTM1 Post Mission Software

YLD_UTM1 was designed to post process the data collected with ***AGYLD1,*** the time tagged yield response of the field. The module for the UTM conversion is used to do the map projection and is not discussed. Several issues had to be addressed in the software in two sections.

Section 1:

- yield sensor and monitor delay
- completeness of yield data string (header sensor, Bu/Ac)
- false readings due to high / low moisture
- speed and heading changes of combine

Section 2:

- data calibration (verified against the true total yield)
- rejection of data at common positions

One of the inherent complications of yield monitoring comes from the method and equipment used to perform the task. In Alberta, a common procedure is to first cut the crop at the stalk and lay a swath of 20 feet or more into a windrow. This

allows the crop to ripen more evenly and puts the crop in a condition that is more resistant to degradation of quality (Goddard, 1994).

The yield monitor has to be set to the proper swath width (varies from farm to farm) for its calculation. There is no means to decipher if a full (i.e., 20 feet) had been swathed or not. For swaths less than 20 feet the yield is lower, which is indistinguishable from a full 20 foot swath that is truly poor yield. Additionally, when the swath is picked up the GPS records the position of the combine, it is not until some time later that the wheat has been separated, traveled up the clean grain elevator and hit the yield monitor's sensor plate. The reading that is being registered by the yield monitor has occurred several metres behind the combine.

Additionally, when the header sensor is up, there is still wheat in the system and the yield monitor is still registering the response. A command line variable delay option allows the user to set the delay time in attempts to minimize the delay effects.

The harvest totals are a function of the monitor system scaled output. The yield monitor coefficients were not

calibrated for each combine and as a result returned quantity readings that were consistently too low. If the true total yield is known from the field (i.e., bin measurement) then the software will calibrate each individual response to sum up to the true value.

The following flowchart outlines the logic to the program in Section 1. In the initial calculations, the calibration factor is set to 1.0 so the results are those recorded directly by the yield monitor. The individual instantaneous measurements of yield will be scaled in Section 2 if a true total harvest quantity is known. The sum of all of the individual measured quantities will be forced to add up to the known value within 5 %. Generally, only 1 iteration is necessary to calibrate the raw yields.

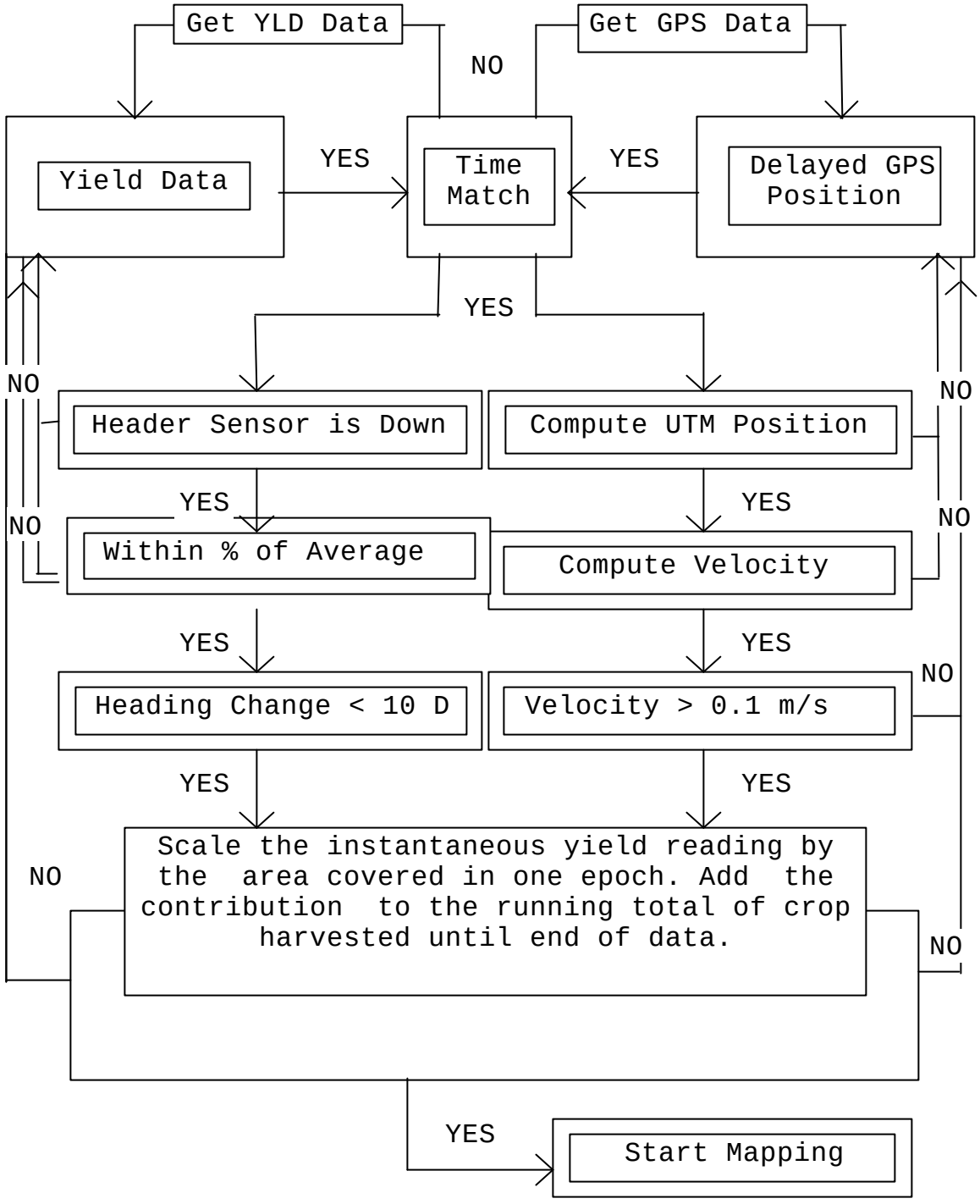

FIGURE 3.2 - Flow Diagram for YLD_UTM1

The total harvest calculation was determined by summing the instantaneous readings during combining. Each Bu per Acre reading recorded from the monitor was then scaled by the true area it represented (based on consecutive position differences multiplied by the swath width), i.e.,

$$T = \sum_{i=1}^{i=n} [\{(DP_i S_i / A) B_i\} s] \qquad (3.7)$$

Where T is the total harvest, **DP** is the grid distance between positions as defined by $((x^{i-1} - x^i)^2 + (y^{i-1} - y^i)^2)^{1/2}$

x, **y** are UTM derived coordinates, **S** is the swath width in meters, A is the number of square metres in an acre (constant), B is the instantaneous bushel per acre output, **n** is the number of samples and s is the scalar calibration factor defined by:

$$s = \frac{\textbf{Known Harvest Quantity}}{\textbf{Calculated Harvest Quantity}} \qquad (3.8)$$

Section 2 consists of a graphical data thinning procedure. The first map point occupation of the UTM derived position, will prevail. Any data that occurs on a re-traveled route (where there is nothing to harvest) will be rejected even though the header sensor may indicate down. The following flowchart illustrates the software logic for Section 2:

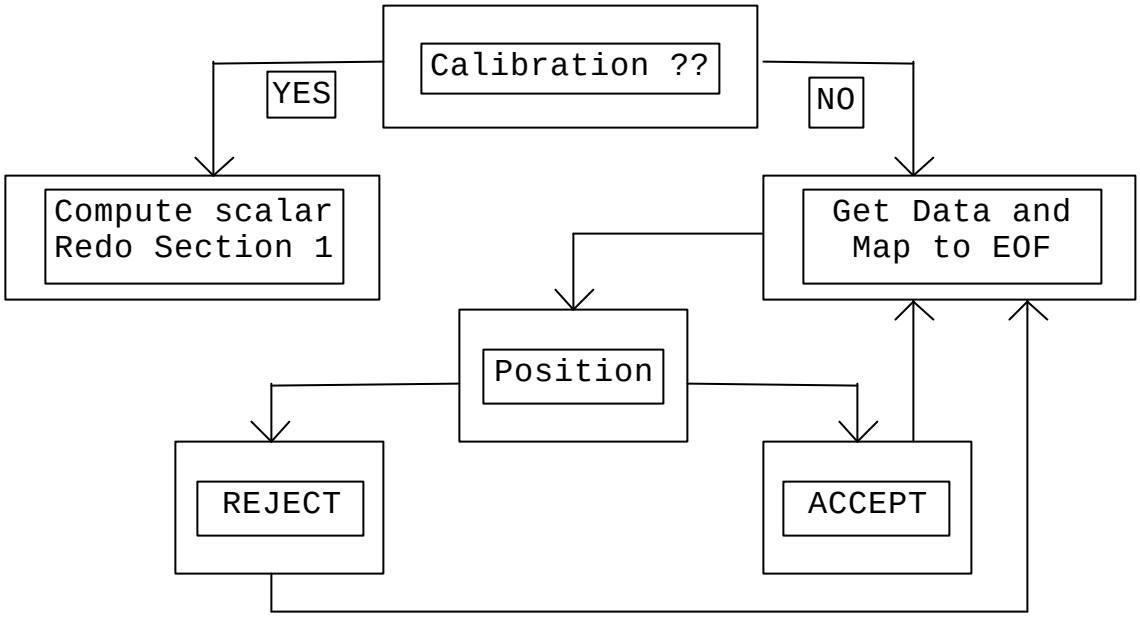

FIGURE 3.3 - Secondary Flow Diagram for YLD_UTM1

Upon the completion of Sections 1 and 2, the resulting data file will be as free from anomalies as currently possible. The data may been rejected for any of the following reasons:

- No GPS position or yield data (i.e. invalid string).
- Header sensor indicates “up” (no crop intake).
- A spike of > 10 % of running average (false readings due to moisture conditions i.e., grain is too heavy or too light as compare to standard weight at 14% moisture content).
- Rapid heading change of > 5 degrees per second (if the field is swathed in a rectangular shape, crop will bunch up at the corners giving false high readings).
- combine movement less then minimum velocity (0.1 m s^{-1})
- Position repeated (yield measurement taken on a first occupation basis).

Of all the software developed for Phase I, ***YLD_UTM1*** requires some fine tuning. Anomalies in the yield maps (i.e., spikes and ridges) indicate that the values recorded and processed are not always indicative of the true crop

behaviour. Experienced agronomists contend that, assuming the field was treated homogeneously, variability exists but changes at a smooth rate, not a rapid jump in a few metres (Myers, 1993).

3.4.3 Salt_UTM1 Post Mission Software

SALT_UTM1 was developed to post process the data collected with the integrated GPS and EM38 conductivity meter using ***AGSALT1***. It uses the UTM conversion module to maintain the common datum and format for input to the GIS at the University of Alberta. The command line option input of the analogue to digital scale factor (see Section 2.5.2) is applied to the EM38 readings and all epoch matching is performed. The data is then formatted and imported into a surfacing routine where the EM38 readings are converted to salinity values (McKenzie et al., 1988) and contoured.

3.5 Development of *FLYVSC3N* and *X_OVER1*

In order to assess the overall accuracy of the DGPS derived positions, it was decided to reprocess selected data sessions using a high precision kinematic approach. The results from the ***OTF*** carrier solution are typically at the centimetre level (Lachapelle et al., 1993) and can be used to assess the ***SC*** position solution. The program ***FLYVSC3N*** was developed for this purpose. Of additional interest was the repeatability of DGPS height component under farming conditions. The accuracy and repeatability of heights for digital terrain modeling, aspect mapping and runoff modeling were was also required to be quantified. The program ***X_OVER1*** was developed for this purpose.

3.5.1 *FLYVSC3N* Post Mission Software

The Program ***FLYVSC3N*** is a command line option, graphical output program that performs an epoch by epoch comparison of any two files sharing the ***SC*** solution output file structure. An option to reject a comparison based on the PDOP value as calculated from the ***SC*** solution is available. The programs

graphical output consists of a histogram summary of the differences followed by a line graph of the epoch by epoch differences. Each graph is titled with the computed RMS value, maximum positive and negative deviations, range of differences, mean value, number of observations and files that were compared.

3.5.2 ***X_OVER1*** **Post Mission Software**

The program ***X_OVER1*** is a command line option program that performs a file search to compare **DGPS** heights at common locations. The following options are:

- Define the HI (same session only). If the 3D DGPS position had not been previously reduced to ground level then it could be accommodated here. To compare sessions from different sessions, the height reduction has to be performed during post processing.
- Define the search radius. Allows the user to select the maximum distance two points can be apart before a comparison can be made. This is very dependent on the vehicle used to collect the data. A combine moves typically 1 - 2 metres per

second while an ATV may travel up to 5 metres per second. The dynamics of the vehicle will influence the choice of the crossover search radius.

- Define the Maximum allowable position dilution of precision (PDOP). Allows the user to reject positions determined under sub optimal geometry to maintain a quality comparison.

The data file to be analyzed is segregated into **X** number of files depending on the range of latitude (m) in the file (i.e., <500 **X**=50, >500 **X**=100 <1000, **X**=200 >1000).

The procedure of dividing the position file into latitude sections is more efficient. Searching is a N^2 operation so if a file contains 50 items it will take 2500 operations to compare all combinations. In the situation of the precision farming project, as may as 36000 positions may exist in a ten hour session. This is 1.2 billion operations which would take approximately 6 days to execute on an AST 486-25 MHz computer if a single file is used. The latitude sections reduce the number of searching operations to the sum of N^2 per file. The processing time is reduced to approximately 2 hours. The efficiency can be further improved by creating search squares

to reduce ***N*** operations per file. However, the size of the search squares or latitude sections can induce potential comparison failures because even though the points are within the search radius, they are in different sub-files. To prevent against this occurring commonly enough to distort the results, the compared positions were later plotted over the trajectory of the DGPS file and inspected graphically.

The approach taken in ***X_OVER1*** has also considered the following assumptions :

- Positions derived under the maximum **PDOP** allowed are then weight equally (distortion due to satellite geometry are not considered).
- The surface around the search point is parallel with the UTM grid coordinate plane. Therefore the height difference is the sum of the errors in the DGPS derived heights plus the true relief difference between the points as illustrated in Figure 3.4.

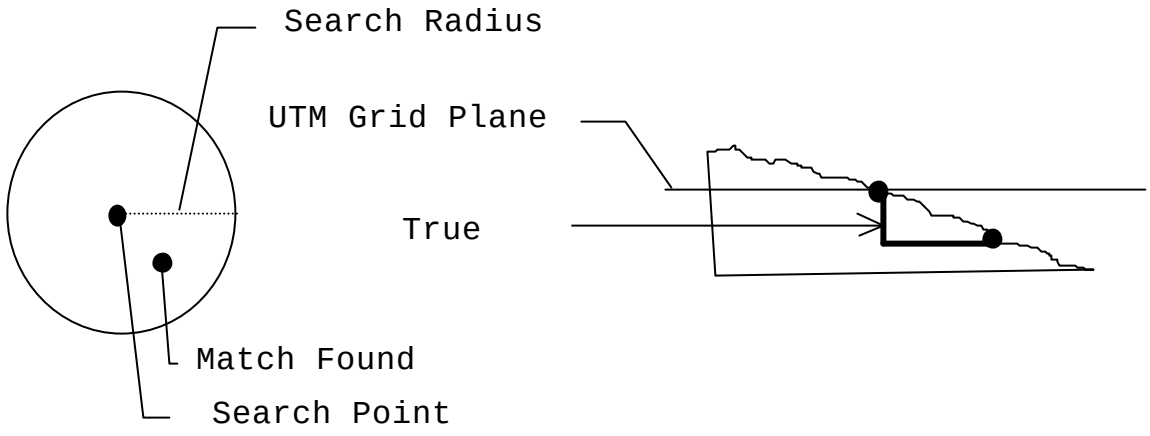

FIGURE 3.4 - Search Radius and Mapping Plane

- The selected ten minutes is sufficiently long to allow time de-correlation between positions.

The graphical program output is a positive half histogram (RMS) summary of the differences titled with the computed RMS value, maximum positive and negative deviations, range of differences, mean value, number of observations and file used.

3.6 Development of Real Time DGPS Software

The engine of the variable rate system for fertilizer input is the navigation system. Without accurate position and

velocity determination in the field, there is no possibility of being able to treat specific parts of the field in any manner. This is one reason fields have always been treated equally in the past. There was no cost effective way to perform the task. The use of **RTDGPS** now offers a solution to the navigation problem. The approach taken was the following:

- Decode, quality check and prepare raw data directly from the ***NovAtel GPSCard***^{TM} simultaneously at the monitor and remote stations for input to **RTDGPS** software. Each station had individual contributions and responsibilities in order to achieve the required differentially corrected position:

At the monitor:

- compute the correction to the pseudorange based on the ***SC*** solution (Eqns. 3.1, 3.2, 3.3)
- compute the rate of change of the correction based on the measured change of the correction between successive epochs
- transmit to the remote station, via radio link, the GPS time and number of corrections to follow

- append the data transmission with the satellite identification number, correction and correction rate for each satellite tracked by the monitor

At the remote:

- search the received data stream of satellites tracked at the monitor with the satellites tracked at the remote and accept common satellites
- compare the transmitted GPS time with the current GPS time and apply latency adjustment to correction
- correct the raw measured pseudorange and solve for the remote antenna position using the ***SC*** solution model (Eqns. 3.1, 3.2, 3.3)

- compute the velocity of the vehicle by using the change of position over time.

3.6.1 Real Time Decoding of the Raw Data

The communication and extraction of selected records from the ***NovAtel GPSCard***^{TM} has already been addressed in the development of ***LOGNOVA1***. All of the raw data integrity checks are maintained. The data string is sent to a function that identifies and decodes it for direct input to the **RTDGPS** solution. Extracted from the data strings are the following:

- satellite I.D.
- pseudorange (metres, L1 only)
- carrier phase (cycles, L1 only)
- carrier phase rate (cycles per second, L1 only)

3.6.2 Calculation of Correction Rate

The parameter required to cancel out the effects of Selective Availability (SA), satellite clock error and minimize the effects of ionosphere and troposphere, which distort the point position by up to 100 metres (2DRMS) horizontally and 150 metres (2DRMS) vertically, is known as a range correction. It is the sum of the intentional dithering and the propagation effects on a per satellite basis. Referring to Eqn. 3.1, the intentional dithering effects of **SA**

are introduced into $\mathbf{d}_r$ and $\mathbf{dt}$ (orbit and satellite clock error) and the propagation effects exist in the $\mathbf{d}_{ion}$ and $\mathbf{d}_{trop}$ (ionosphere and troposphere, Section 3.1),

It is computed by comparing the calculated range (based on a fixed monitor station, computed satellite position (**R**) to the measured range (***P,*** Eqn.3.1). The difference (including measurement noise) is the magnitude of the single point GPS error on that satellite. If the monitor - remote baseline is less than 5 km, as is the case in this project, then the magnitude of the error is highly correlated for both stations. The correction is applied by subtracting the it directly from the range computed at the remote station. the remote station can then compute its differential position with respect to the monitor.

The assumption made in computing the remote station differential position is that both receivers acquire and decode the raw data simultaneously. The range correction computed at the monitor station is not directly applicable to the remote because by the time it is transmitted and received it applies to the previous epoch not to the current epoch.

The problem is known as data latency. It can vary from the data collection rate to tens of seconds based on the transmission method (i.e., cellular modems can take as long as 30 seconds to complete data transmissions, Falkenberg et al, 1992). Figure 3.5 demonstrates the correction variation over time. Plotted is the magnitude of the range correction in the presence of **SA** for satellite 17.

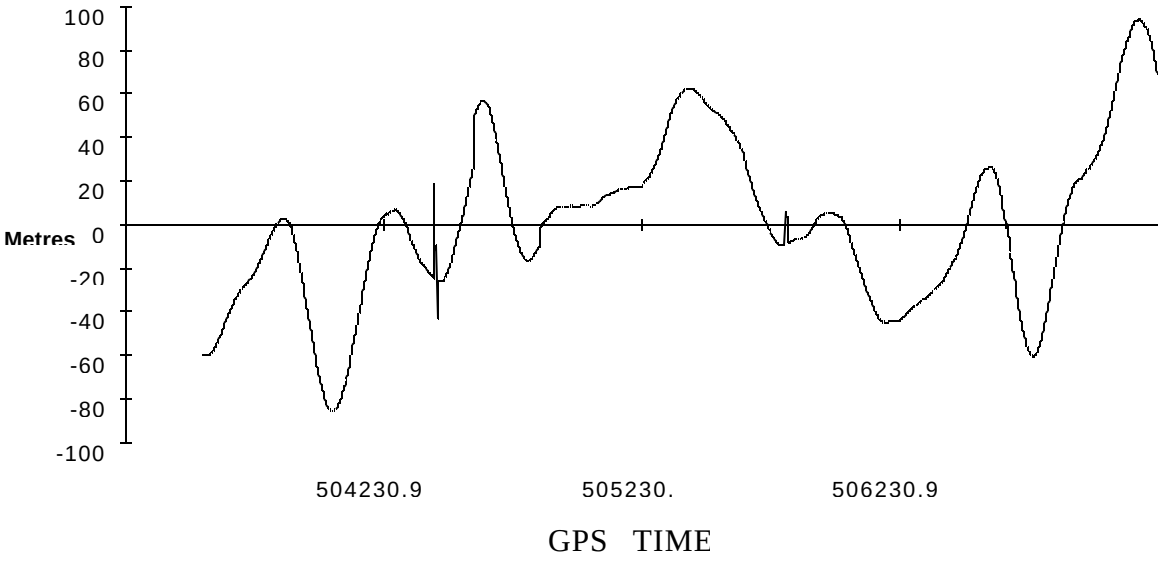

FIGURE 3.5 - Range Correction Variation Over Time

The plot above indicates that the behaviour of the range correction mimics SA. This is expected because SA is the largest component of the range error (Hofmann - Wellenhof, 1992). If line integral is broken into differential elements of sufficiently small enough size (i.e., dx elements) then a linear approximation can be made. Figure 3.6 below illustrates the correction behaviour over a shorter time period.

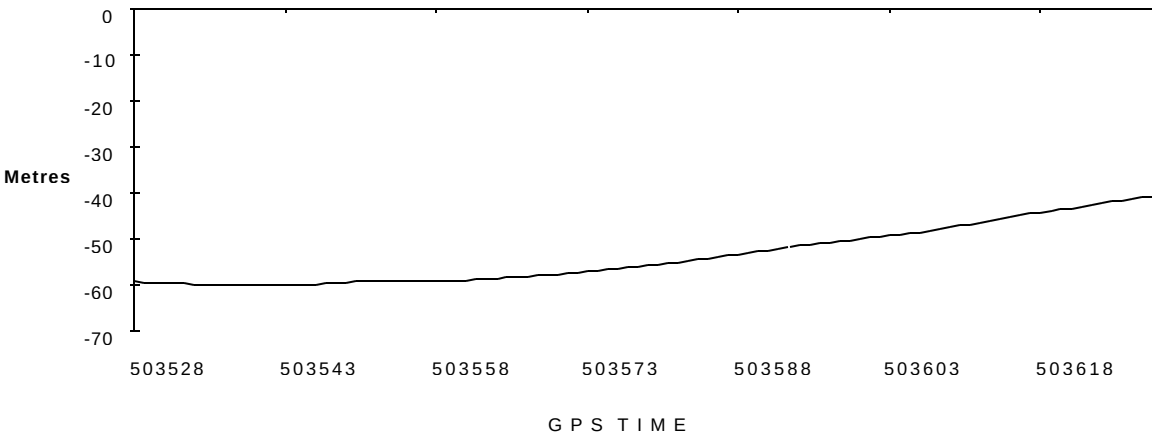

FIGURE 3.6 - Correction Variation - 100 Second Period

If the correction is detracted even farther in time to a 20 second window, it appears to be linear.

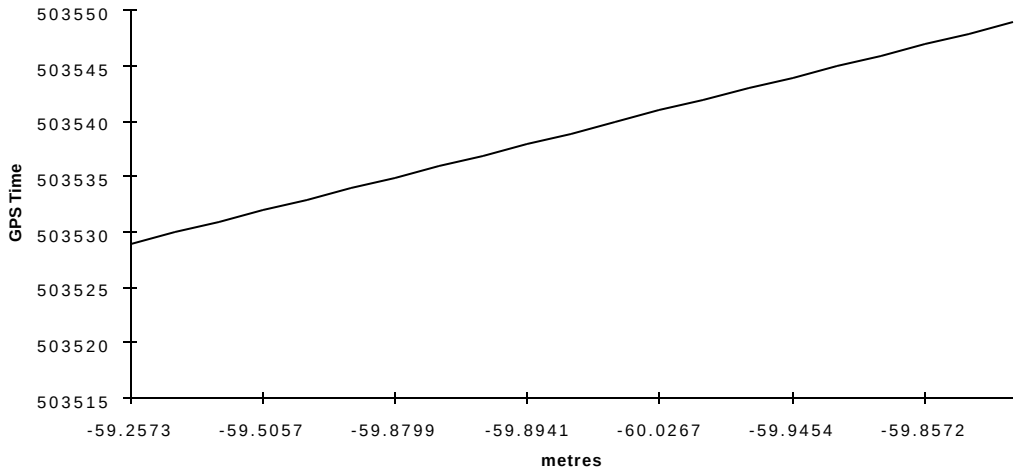

FIGURE 3.7 - Correction Change - 20 Second Period

Based on the behaviour of the change of the correction over a short time period, the most reactive approach to computing the correction rate is to take the change over a single epoch. This way an acceptable linear fit can be made. The slope of the approximation will also change instantly with the change in **SA** on a per satellite basis. The correction rate was computed in the following manner:

$$\dot{dr} = \frac{dr^{i} - dr^{i-1}}{T^{i} - T^{i-1}} \qquad \textbf{(3.9)}$$

where $\dot{dr}$ (m/s) is the rate of change of the correction, dr, dr^{i-1} (m) are the range corrections over subsequent epochs and T^{i}, T^{i-1} (s) are the GPS times at the present and previous epochs. This approach can experience distortions if a severe change of geometry occurs between the epochs. Another approach is to use the observed Doppler shift scaled to range rate (Hoffman-Wellenhoff et al., 1993). This method is more robust as the Doppler is an independent measurement at each epoch.

3.6.3 Computation of the Latency Correction

To deal with the distortions of latency, the range correction must be predicted using the rate of change and the latency in a linear prediction equation. The prediction of the correction was computed in the following manner:

$$\hat{dr} = dr + \dot{dr}\,DT \qquad \textbf{(3.10)}$$

where $\hat{dr}$ is the predicted value of the correction, dr is the current correction value, DT is the latency of the correction and $\dot{dr}$ is the computed range rate (Eqn. 3.9).

The computed prediction is then used to adjust the smoothed pseudorange at the remote station and compute a differentially corrected position.

3.6.4 Computation of Velocity

The velocity of the tractor is required for the rotation period defining the fertilizer flow rate. If a constant flow rate is required then the servo motor rotational speed will be a function of the tractor velocity. It will have to rotate faster to output the same mass of material in the same area if the tractor velocity increases creating an increase in ground coverage.

Computation of the tractor velocity was performed by computing the change in position over time. This allows for mean velocity between differentially corrected positions even if epochs are missed due to failure to receive corrections. The three dimensional **DGPS** position was used to allow for travel on hilly ground. The following methodology was used:

$$\dot{r} = \frac{\sqrt{(X^{i} - X^{i-1})^2 + (Y^{i} - Y^{i-1})^2 + (Z^{i} - Z^{i-1})^2}}{T^{i} - T^{i-1}} \qquad \textbf{(3.11)}$$

where $\dot{r}$ (m/s) is the velocity in the position domain, ***X,Y,Z*** *are* Earth centred Earth Fixed (ECEF) GPS coordinates (m), T^{i}, T^{i-1} (s) are times at the current and previous epochs.

3.7 Variable Rate Application

Variable rate application instruction is possible via the prescription map designed by soil scientists and agronomists based on the data analysis of Phase I. Using a GIS, surfaces depicting yield, salinity, topography, soil types and nutrients are overlayed. Regions are identified and RT DGPS navigation provides the position required for variable rate application for crop optimization or test banding to further study the crop response.

3.7.1 Prescription Map Data Base

The instructions for custom fertilizer application are encoded in the prescription map data base. The data base information is divided into two separate sections. Section 1 is for map management,coordinate extent, cell deliniation and parameter definition. Section 2 contains the coded rate per fertilizer type and bin allocation. The first ASCII code character pertains to front bin while the second pertains to the back bin.

Section 1 :

- Line 1: File name (for field identification)
- Line 2: UTM easting, northing for the NW corner of the map (cell[0][0], number of cells east and south, size of cell (in metres) east and south
- Line 3: Nitrogen input codes (10 channels, Lb per Ac)
- Line 4: Phosphorus input codes (10 channels, Lb per Ac)

Section 2:

The prescription map instructions are in an ASCII map format. The UTM position, size and resolution of the map are defined by line 2 in Section 1. The number of cells east and south set the map boundaries and the size of each cell sets the UTM coordinate extent of the map. Any positions outside the map boundaries are not acknowledged. The data base was developed so that the prescription maps could have variable resolution in both UTM directions to best fit the field shape.

Each cell has two single digit integers (0-9) that correspond to a rate input as per line 3 or 4 in Section 1. The first is the nitrogen input followed by phosphorus. Below is an extract of the Stettler database in ASCII map format:

```
24242424242424242424242424242424242424242424242424242424
24242424242424242424242424242424242424242424242424242424
24242424242424242424242424242424242424242424242424242424
24242424242424242424242424242424242424242424242424242424
24242424242424242424242424242424242424242424242424242424
44313124242727242420202727242420204444242424242424242424
44443131242427272424202027272424202044442424242424242424
34444431312424272724242020272724242020444424242424242424
34344444323224242727242420202727242420204343242424242424
```

Figure 3.8 - Prescription Map - ASCII format

This information is then communicated to the variable rate hardware (Section 2.6.2) and performed at this location in the field.

3.7.2 Data Base Searching Technique

With the computation of the DGPS position converted to the UTM coordinate plane, the task of extracting the blend and mass volume of inputs is to be accomplished. The searching process is performed in two steps:

- determine which cell represents the tractor’s position

- extract the two single digit codes for nitrogen and phosphorus and convert them to input rates

The prescription map was resident on the hard drive of the computer and had to be physically scanned to the correct location for the extraction of the input digits. Each row was classified as one large string (i.e., a sentence). The number of strings to scan through was defined as the integer difference between the UTM northing of the tractor and the UTM northing of the N.W. corner of cell[0][0]. The number of characters in to the sentence was defined as the integer difference between the UTM easting of the tractor and the UTM easting of the N.W. corner cell[0][0]. The computation also considers the possibility of non uniform cell sizes. The result is the cell location cell[i][j] as defined by:

$$i = \frac{UTM(N)_{oo} - UTM(N)_{Tractor}}{UTM(CellSize)_{north/south}} \qquad \textbf{(3.12)}$$

$$j = \frac{UTM(E)_{oo} - UTM(E)_{Tractor}}{UTM(CellSize)_{east/west}} \qquad \textbf{(3.13)}$$

where $UTM(N)_{00}$ and $UTM(E)_{00}$ are the reference UTM coordinates of cell[0][0], $UTM(N)_{Tractor}$ and $UTM(E)_{Tractor}$ are the derived UTM coordinates of the tractor, $UTM(CellSize)_{east/west}$ and

$UTM(CellSize)_{north/south}$ are the cell dimensions in the respective grid directions.

The **RTDGPS** program initialized a search that scanned in "i" strings and extracted out characters "j", "j^{+1} from the string and converted them to field inputs.

3.7.3 Variable Rate Flow Rate Determination

The first two steps in variable rate fertilizer applications have been completed. The last step is to perform the requested action. The **MCU** servo motor interface requires the rotational periods for each motor base on the following:

- the velocity of the tractor (Eqn. 3.11)
- the required mass inputs for each fertilizer (cell[i][j] and cell[i][j+1] (Eqn. 3.12, 3.13)

The periods are then computed and sent to the MCU for analogue conversion and servo motor action.

3.7.4 Flow Rate Calculation

The rotational period for each motor dictates the mass of material dispensed into the airseeder wind tunnel and out through the implement into the ground. Two constant values come from the calibration of the air seeder:

- The base period (***Base***) - the period of one revolution at 100 RPM
- The Mass Per Revolution (***MPR***) - Mass dispensed by one revolution of the servo motor.

The computation is performed in three steps:

- Acres Per Minute (*APM*),

$$APM = \frac{\dot{r}}{60} \cdot 5280 \cdot DW \cdot \frac{640}{5280^2} \qquad \textbf{(3.14)}$$

where $\dot{r}$ is the velocity converted to MPH, **60** is the number of minutes in an hour, **5280** is the number of feet in a mile, ***DW*** is the drill width in feet, **640** is the number of acres in a square mile.

- Revolution per Minute (***RPM***),

$$RPM = \frac{Rate}{MPR} \cdot APM \qquad \textbf{(3.15)}$$

where ***Rate*** is the prescription map value.

- Period (***P***),

$$P = \frac{100}{RPM} \cdot Base \qquad \textbf{(3.16)}$$

All of the computations in this chapter were performed over a period of one second and communicated to the variable rate applicator (Section 2.6.2) for action.

CHAPTER 4

RESULTS OF PHASE 1 AND GPS PERFORMANCE

The Phase I data campaign occurred from August to November, 1993. Post processing, mapping and analysis of the data confirmed that variability exists. The DGPS integrated systems used to collect field attributes gave the researchers with maps of yield, salinity, soils, nutrients and elevations at a resolution and data density never achieved previously. When converted to a raster based map format they can be layered via a GIS package (i.e., GRASS) for further analysis. The accuracy and reliability could also be assessed based on the post processed results.

Figure 4.1 shows the distribution of the test sites in Alberta. Figures 4.2,4.3,4.4 and 4.5 are a sketches of the general field shapes with a brief summary of data collected from each site during the Phase I data campaign .

4.1 Site Selection

To perform research at farm scale four sites within Alberta, operated by Farmer Cooperators, were selected that represented a range of farming conditions throughout the province. Each site has different agro-ecological features. Selection criteria included moisture regime, salinity, soil types and topography.

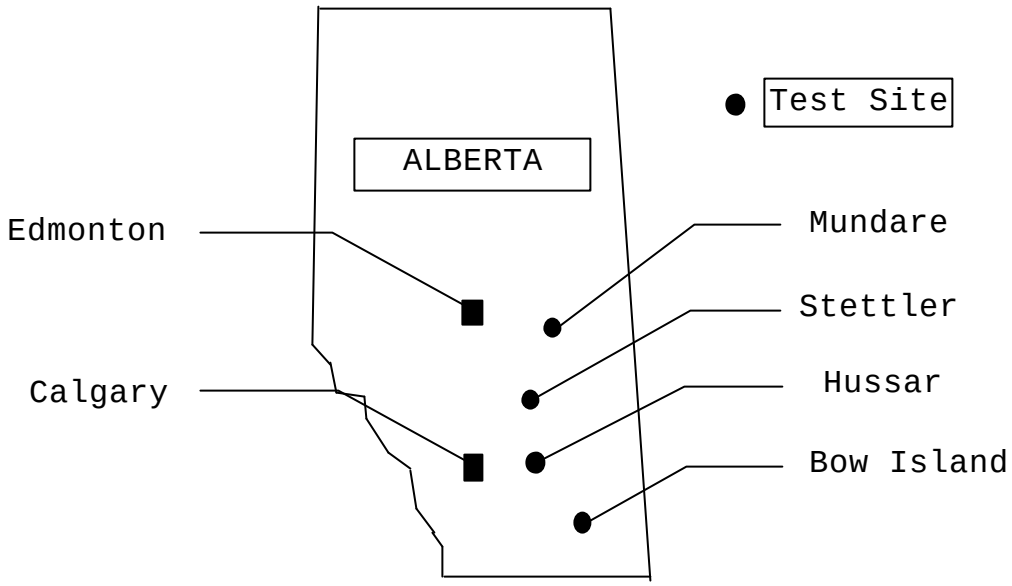

Figure 4.1 - Location of Farm Sites

4.1.1 Bow Island

Bow island is 130 acres under a centre pivot irrigation system. Seeded to wheat, it experienced large quantities of volunteer barley. Salinity problems exist on the gradual sloping topography of approximately 8 metres in relief. Brown soils with silty loam exist on till and fluvial parent material. Data on yield, salinity and soils were collected.

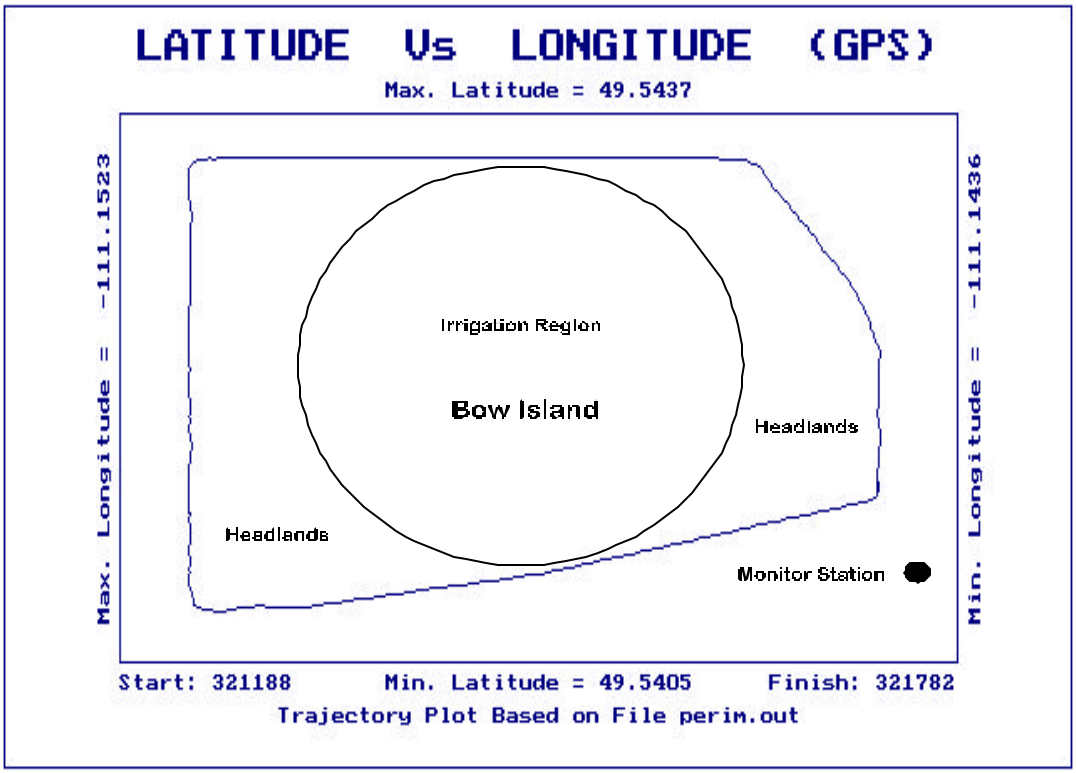

FIGURE 4.2 - Bow Island Test Site

4.1.2 Hussar

Hussar is a 200 acre field of spring wheat dominated by a large hill. Relief is approximately 40 metres with smaller hills around the perimeter. The field has experienced long duration cultivation which resulted in a soil erosion problem while some land has been recently broken out of native grass. Dark brown soils and clay loam exist on till parent material with calcareous on eroded hilltops. Data for truthing transects, yield and soils were collected.

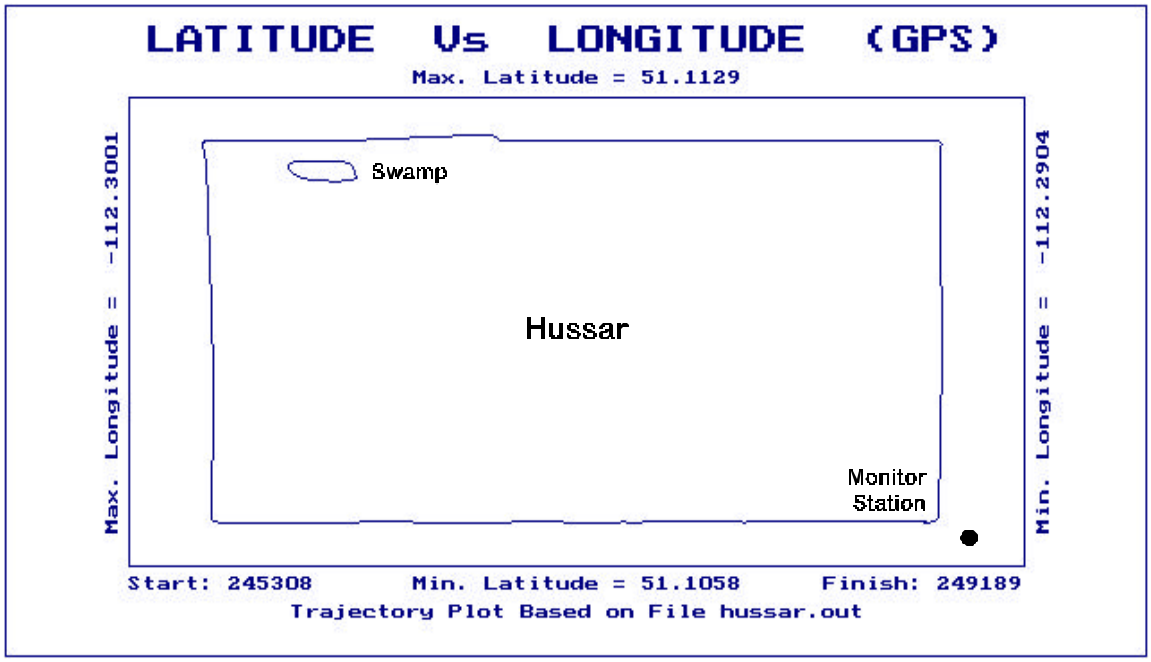

FIGURE 4.3 - Hussar Test Site

4.1.3 Stettler

Stettler is an 80 acre field seeded to Harrington barley. It has extremely hummocky topography with knolls of approximately 5 to 10 metres relief. The black soils have fluvial and till parent materials and topsoil textures range from loamy sand to loam. The field has been cultivated for 80 years with a crop rotation of barley, barley, wheat, canola cycle. Data on yield and soils were collected.

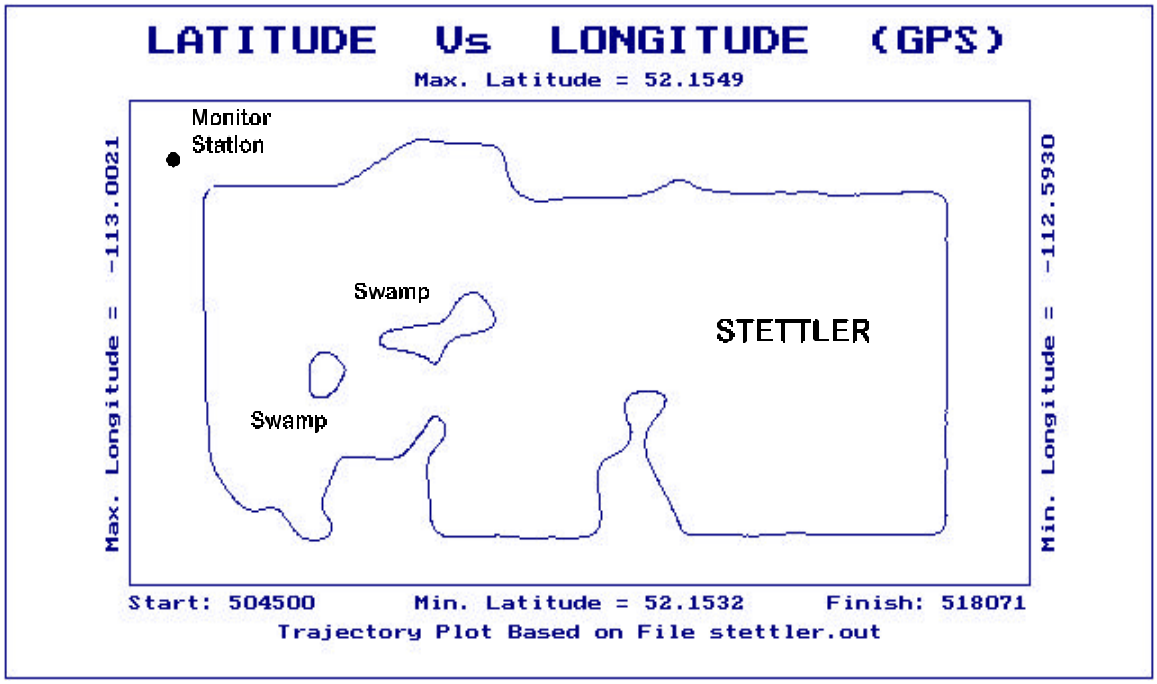

FIGURE 4.4 - Stettler Test Site

4.1.4 Mundare

Mundare is an 80 acres field that is part of the Parkland Agriculture Research Initiative (PARI) site. The experimental field was seeded with canola. The landscape is a low relief, hummocky till plain with potholes of low lying regions not suitable for farming. The black soils have predominately silt-loam textures and are affected by salts and impermeable subsoil. Data on TDR probe results, square metres cuts, salinity and soils were collected.

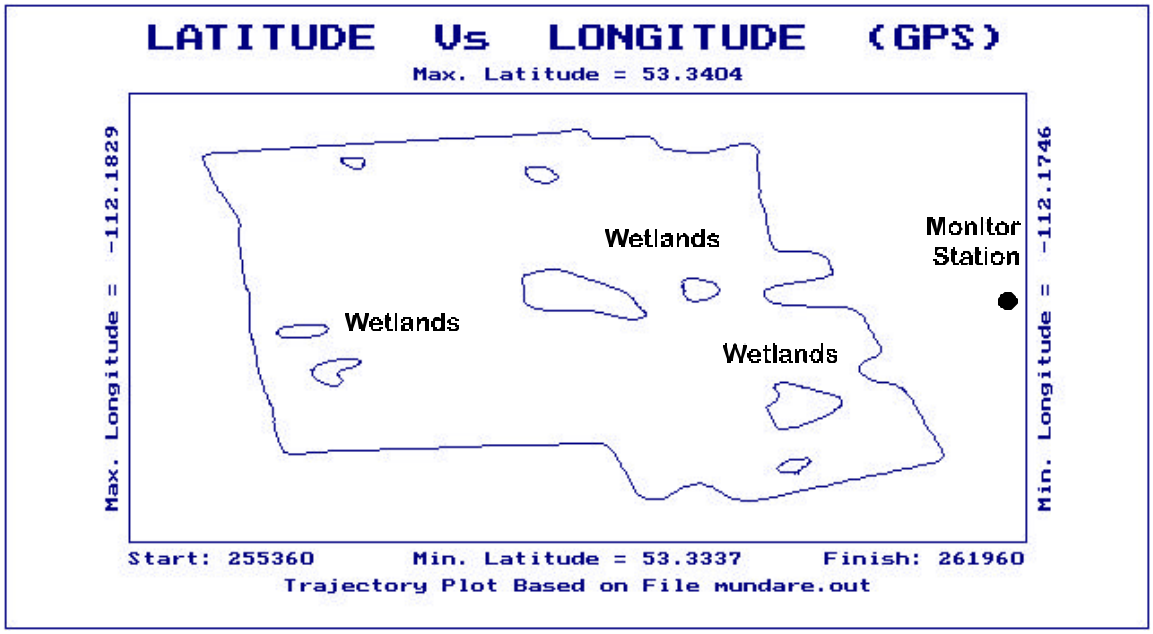

FIGURE 4.5 - Mundare Test Site

4.2 Harvest Results (*YLD_UTM1*)

Only three of the four selected sites were harvested in Phase I. The Mundare site was neglected due to a problem with the hardware required for the yield monitor. The three remaining sites, Bow Island, Hussar and Stettler were successfully harvested. The yield response from Bow Island was not as extreme as at the other two sites. This is due to the extensive control over moisture and the lack of relief across the field. The two remaining sites showed that extensive variability exists and only the relative magnitude is different for each field.

Figure 4.6 shows the combine track and yield measurement (in gray tone scale) for the Hussar site. At this site two combines were used due to the poor weather forecast. Only every other swath was measured for yield. The output from ***YLD_UTM1*** (Sec. 3.4.2) overlays the crop response at each DGPS position so that variability can be inspected visually across the field. This allows researchers to isolate select parts of the field for closer analysis (the program ***SORT_YLD*** allows direct data extraction primarily for this reason). The mottled appearance of the spatially related data in the figure below illustrates the extent of the variability found in the field.

Several patterns of crop response can be seen based on the history and landscape knowledge of the site.

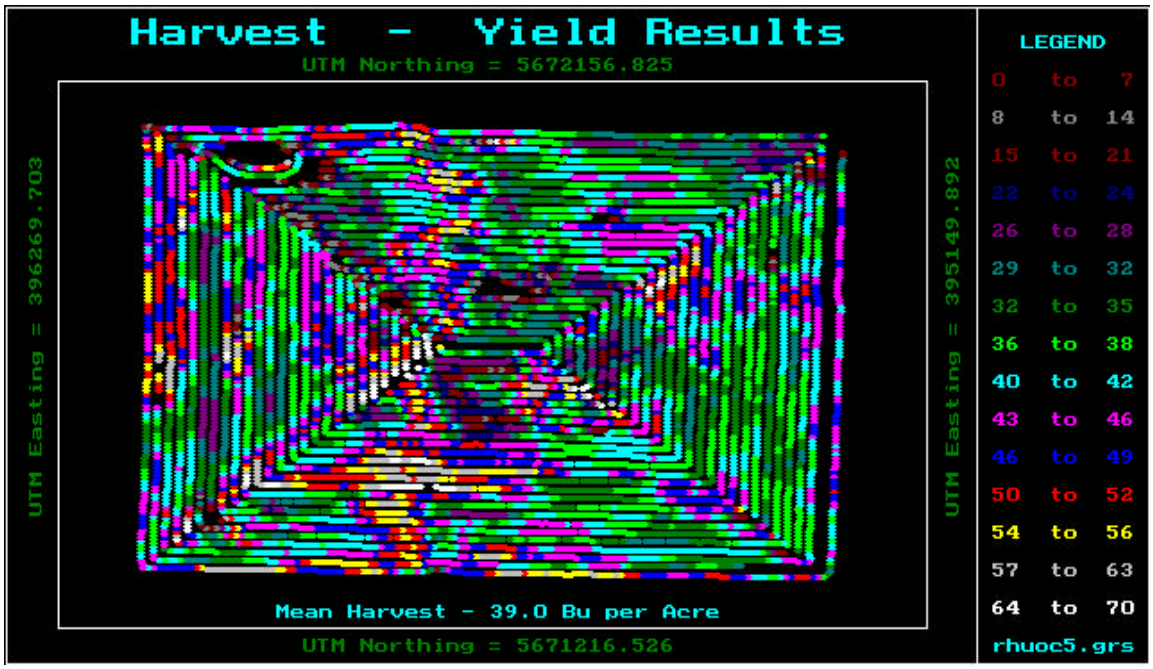

FIGURE 4.6 - Hussar Harvest Response

The variability is due to the inherent differences in soil, nutrients, landscape, salinity and history of the field. What is to be yet determined is the extent that each factor has on crop response and how it should be dealt with at pre-seeding and seeding time. This is a task for the agronomists and soil scientists. However they do now have at their

disposal vast amounts of spatially related data to assist them in their analysis.

4.3 Salinity Results (*SALT_UTM1*)

Although automated data collection for salinity mapping is not new to the agricultural industry (Lachapelle et al., 1992), improvements in the integrated system had been made. The position accuracy of the EM38 data has been improved by moving to a high performance **GPS** receiver. The degree of salinity in any given field can have a significant effect on crop response (McKenzie et al., 1989). The following figure is a salinity survey performed at Mundare and the resulting salinity map. This map can also be overlaid on other field information for further analysis.

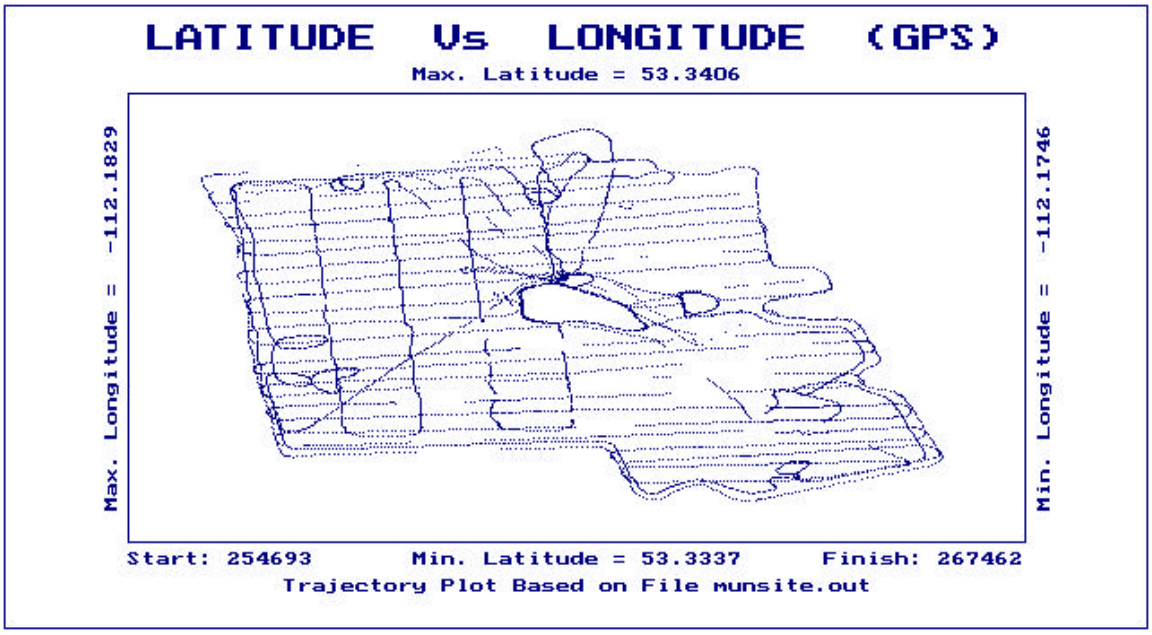

FIGURE 4.7 - Data Points for Salinity Map

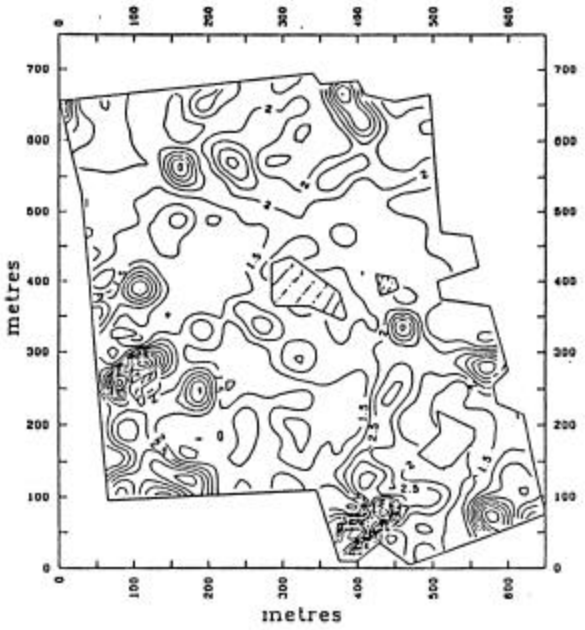

FIGURE 4.8 - Salinity Map of Mundare

4.4 DGPS Accuracy and Repeatability in Height

A concept to research is the accuracy and integrity of the results that are used to base actions. The results of the crop response and salinity mapping can be ground truthed History of the field use and soil sampling have been well documented by the farm operators. What is left to confirm is that the position information that has been collected via the integrated systems is sufficiently accurate for the intended purpose.

To assess the quality of the DGPS data for the entire project, several of the larger data sets were re-processed using a technique different than the ***SC*** solution approach. A high precision kinematic processing run was performed using the ***OTF*** (Section 3.2) phase solution. The developed ***FLYVSC3N*** (Section 3.5.1) was used to perform epoch by epoch comparisons. The **OTF** phase solution approach had to be taken because there existed no other way to resolve the ambiguities. No antenna swap or fixed baseline initialization procedure preceded any of the campaigns.

To further investigate the height component, used for DTM and associated derivatives of surface modeling, a height repeatability analysis was performed using the developed software ***X_OVER1*** (Section 3.5.2). The results of both the ***SC*** solutions and the ***OTF*** phase solutions are assessed.

4.4.1 ***FLYVSC3N*** Results

The **OTF** solutions, used to assess the **SC** performance, were verified as correct by inspecting the residuals of each solution. Typically, the RMS values were less than 3 cm for all satellites used in the solution. The time required to resolve the integer ambiguities was between 5 to 15 minutes depending on the number satellites that were being tracked which was between 5 and 10 for the project.

Two of the largest data sets spanning two day periods, and a four hour data set were used to assess the position accuracy of the **DGPS** in ***SC*** mode. At all times a choke ring was used at the monitor station but due to mounting constraints, one was not used on the remote. The following data sets were used:

- the Hussar swathing data (September 20,21, ses. 1,2,3,4)
- the Hussar soil sample location data (November 9, ses. 5)
- the Bow Island harvest data (September 30,31, ses. 6,7,8)

The swathing and harvest data sets were collected during normal farming operations where as the soil location data set was extended to perform a grid pattern for the testing of height repeatability. Shown below is the tractor trajectory of the Hussar site (session 1-4). Data was collected at 1 Hz with more than 70,000 position comparisons made.

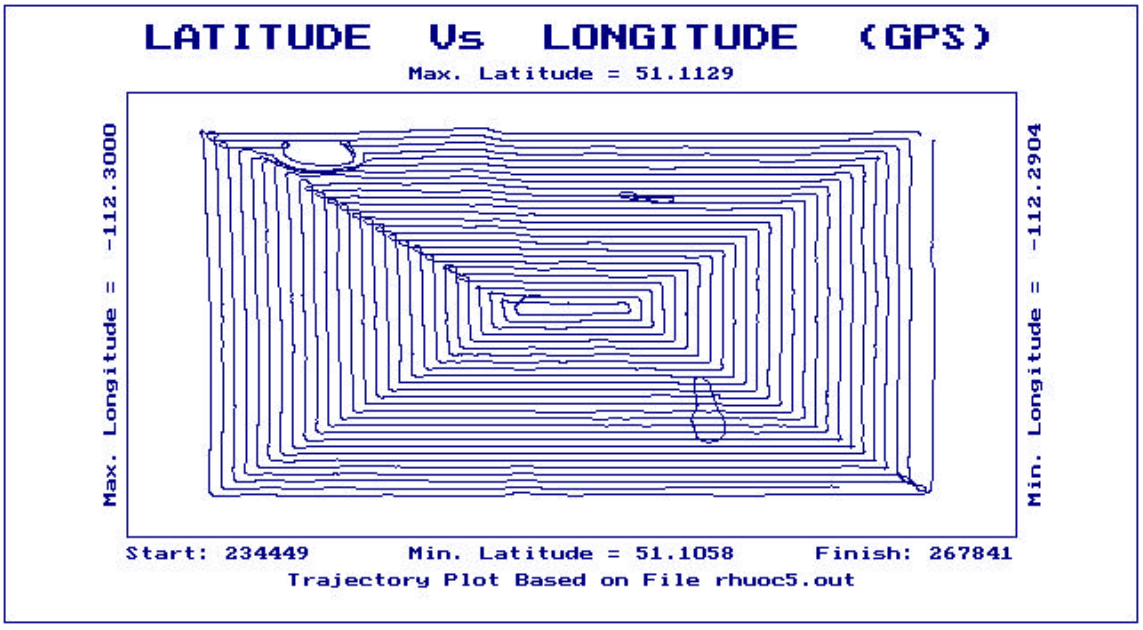

FIGURE 4.9 - Trajectory Plot for September 20-21

The following histograms (Ses. 5) illustrate the typical range of the differences experienced at all sites.

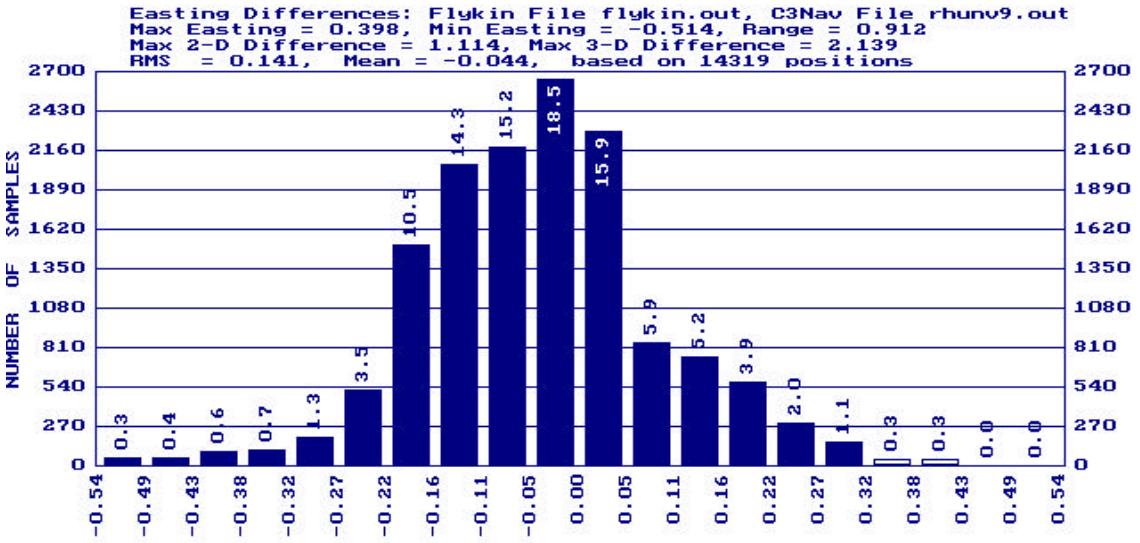

FIGURE 4.10 - Histogram of Easting Differences

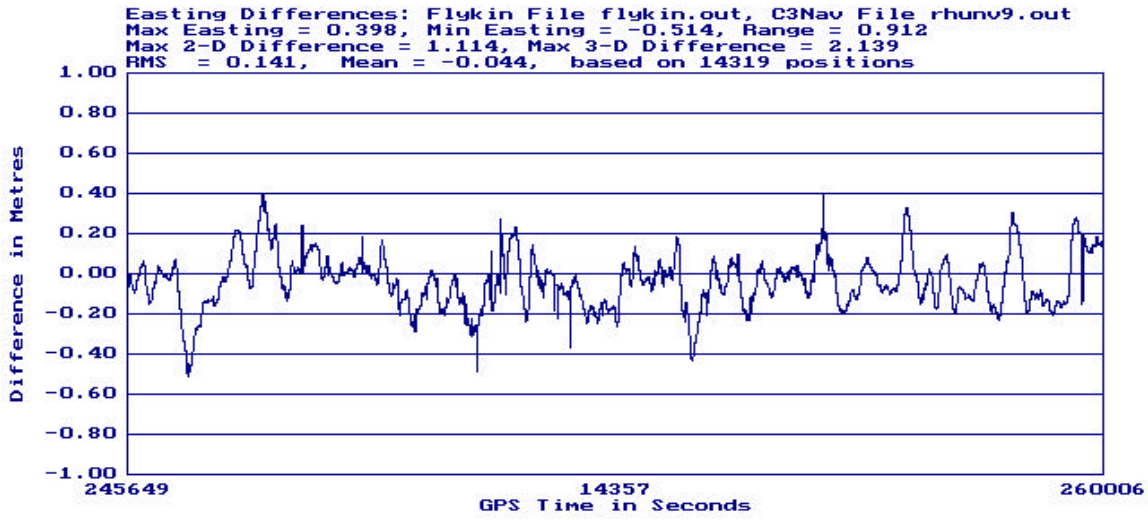

FIGURE 4.11 - Epoch by Epoch Comparison

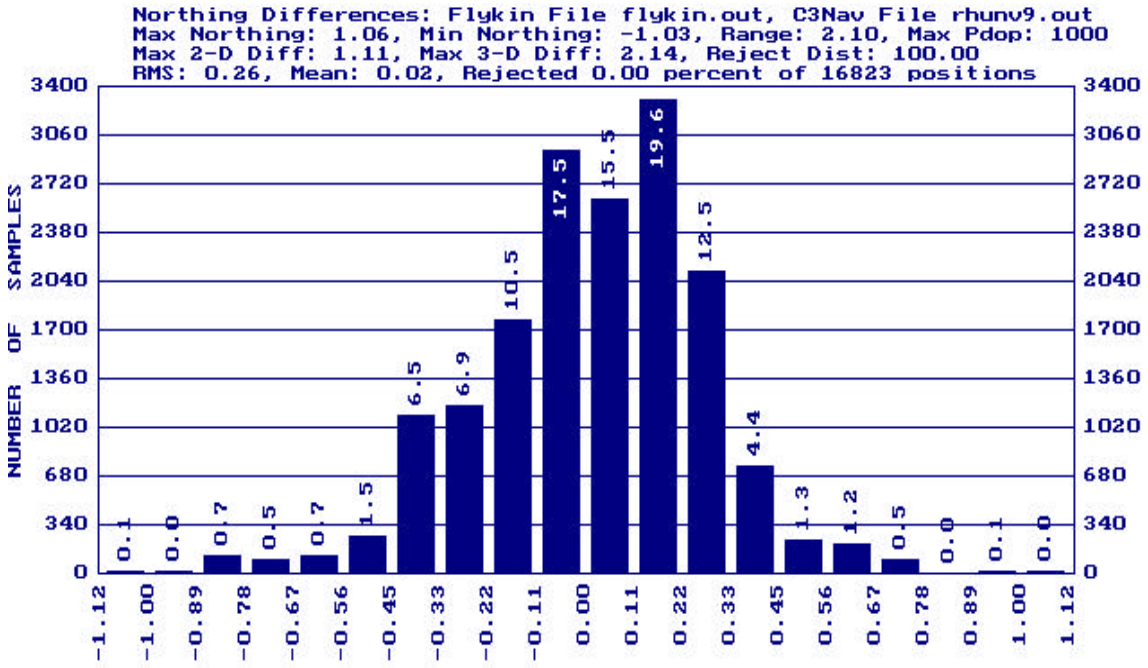

FIGURE 4.12 - Histogram of Northing Differences

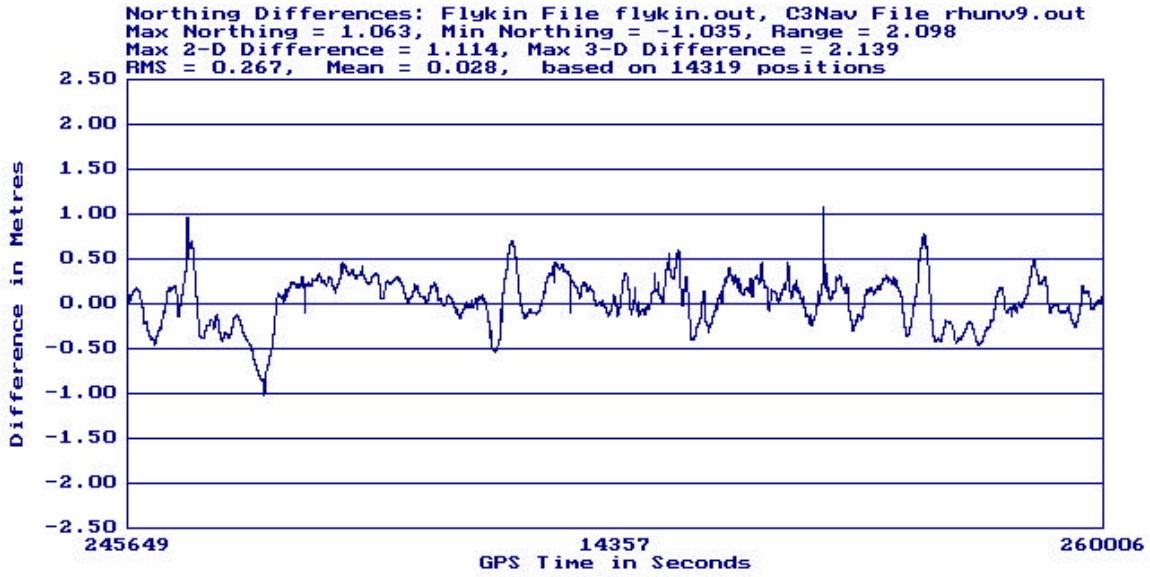

FIGURE 4.13 - Epoch by Epoch Comparison

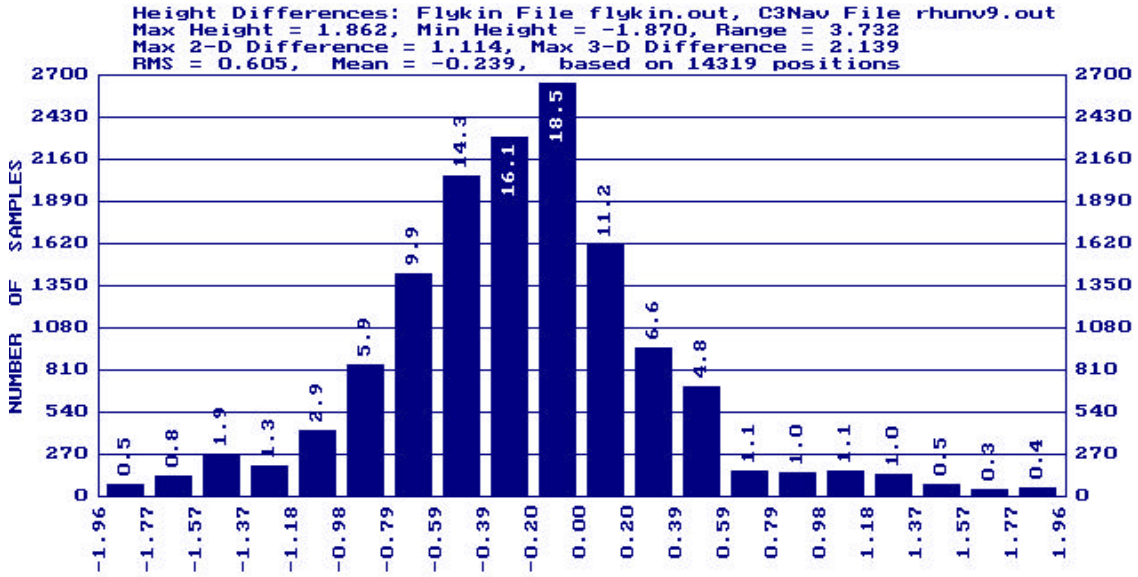

FIGURE 4.14 - Histogram of Height Differences

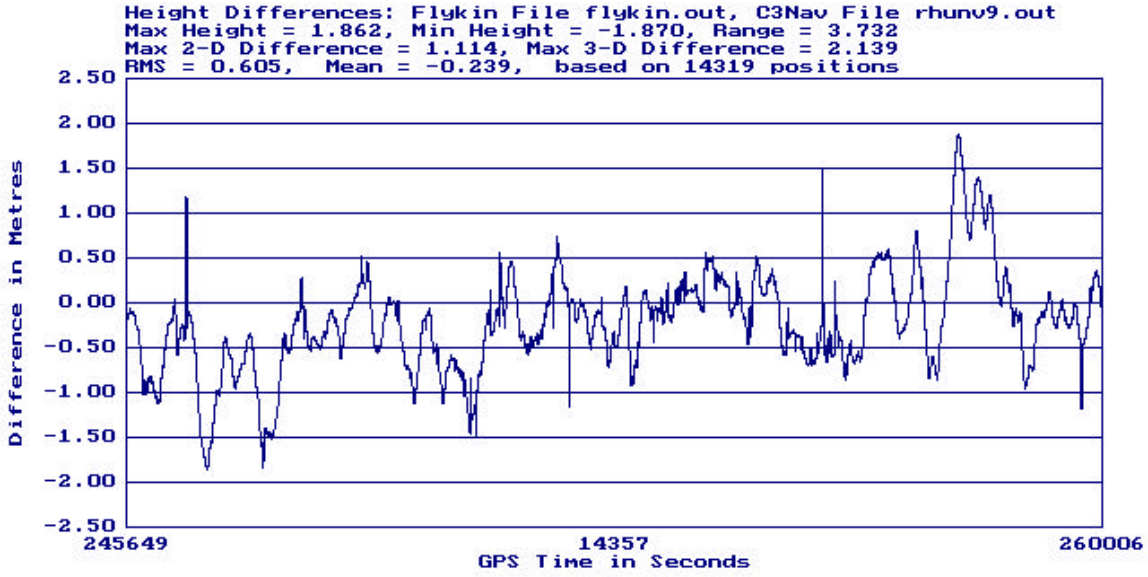

FIGURE 4.15 - Epoch by Epoch Comparison

The histograms indicate that the differences in UTM easting, northing and height are distributed normally. The epoch by epoch line plots show the classic sinusoidal low frequency trend of multipath. In this case it is a combination of ground multipath and multipath created by the combine itself. No choke rings were used on any of the remote stations in attempts to minimizing multipath due to mounting constraints.

The spikes in the line plots are due to changes in **PDOP** values which magnify the error in the code position capabilities. This commonly occurs when a satellite is blocked or the data is rejected causing a sudden change in the satellite constellation and hence **DOP**. A maximum **PDOP** value of 10, calculated by the ***SC*** solution, was used as a rejection criteria for a position comparison.

The high frequency noise is a combination of the receiver noise on the code and the receiver noise on the phase. When you combine solutions, the noise associated with each solution is carried onto the result. In this direct epoch by epoch

comparison, the ***OTF*** phase solution is taken to be errorless which in reality is not true. Residual effects of multipath in the 2-3 cm level and measurement noise in the cm level are still resident in the solution (Evans, 1986).

The table of position results is therefore a pessimistic estimation of the true results because they include the residual errors of the ***OTF*** phase solution.

Desc.	Start	End	RMS	Max	Min	Mean	Obs.
Ses 1	59830	77610					14386
E			0.171	0.355	-0.588	-0.085	
N			0.249	0.736	-1.043	-0.074	
H			0.583	0.851	-1.844	-0.401	
Ses 2	89583	89660					3678
E			0.123	0.246	-0.349	-0.074	
N			0.135	0.290	-0.315	0.046	
H			0.482	0.013	-0.291	-0.417	
Ses 3	248795	253505					4674
E			0.103	0.207	-0.770	0.025	
N			0.143	0.435	-0.393	0.080	
H			0.405	-0.017	-1.137	-0.369	
Ses 4	256829	266380					9458
E			0.145	0.438	-0.291	0.019	
N			0.194	0.500	-0.356	0.111	
H			0.450	0.629	-1.388	-0.325	

Table 4.1 - Hussar Swathing Data - Results in Metres

Desc.	Start	End	RMS	Max	Min	Mean	Obs.
Ses. 6	245650	260006					14319

E			**0.141**	**0.398**	**-0.514**	**-0.004**	
N			**0.267**	**1.063**	**-1.035**	**0.028**	
H			**0.605**	**1.862**	**-1.870**	**-0.239**	

Table 4.2 - Hussar Soil Data - Results in Metres

Desc.	Start	End	RMS	Max	Min	Mean	Obs.
Ses 6	**441125**	**452300**					**11118**
E			**0.180**	**0.970**	**-0.511**	**0.024**	
N			**0.210**	**0.780**	**-0.817**	**0.044**	
H			**0.411**	**1.183**	**-1.807**	**0.103**	
Ses 7	**409700**	**506000**					**9063**
E			**0.110**	**0.482**	**-0.431**	**-0.007**	
N			**0.146**	**0.842**	**-0.782**	**0.024**	
H			**0.349**	**2.698**	**-1.333**	**-0.001**	
Ses 8	**535000**	**538500**					**3499**
E			**0.247**	**1.738**	**-0.175**	**0.119**	
N			**0.208**	**0.291**	**-1.798**	**-0.014**	
H			**0.579**	**0.828**	**-4.099**	**-0.078**	

Table 4.3 - Bow Island Combine Data - Results in Metres

The mean RMS values (1σ) of the data sets are 0.112 m, 0.194 m and 0.477 m for the easting, northing and height components respectively based on 70,195 position comparisons. This surpasses the project RMS accuracy requirements of 0.5 m horizontally and 1.0 m vertically. To further enhance the DTM

modeling and aspect mapping capabilities, the cm level ***OTF*** phase solution used.

The position results are an indication of the advances in receiver technology. The narrow correlator spacing technique produces accuracies reliably in the sub metre range in 3D. A standard correlator receiver (chip length of 293 metres) produces position accuracies in the 2-5 metre range. The differences in the price of the hardware may or may not justify the higher accuracies for a commercial market. For may aspects of the project, less than 5 metre accuracy is acceptable (i.e., soil sampling) but totally inaccurate for yield monitoring.

4.4.2 ***X_OVER1*** Results

The verification of heights determined from DGPS was required to quantify the errors in the DTM and associated offshoots of surface modeling. The height component of DGPS is the weakest part of the derived 3D position. This is because

only the upper hemisphere of the constellation is visible for the user and hence there is only geometric strength in the up direction. Latitude and longitude are more accurately derived due to stronger geometry in east/west and north/south directions. This is evident when inspecting tables 4.1 to 4.3 of Section 4.2.1. The RMS values significantly increase for the height component as compared to the RMS values for the latitude and longitude generally by a factor of 2.

The program ***X_OVER1*** (Sec. 3.5.2) was designed to determine the repeatability in the height component in a data campaign or an inter-session comparison. To be able to make an adequate investigation all data to be tested must be at the same height datum (i.e., ground level). Two tests were conducted using the following data sets:

- the Hussar swathing data (September 20,21)
- the Hussar soil sample location data (November 9)

The November 9 data campaign was tested for an internal determination of repeatability. Below is the trajectory plot of the grid pattern used. Each dot on the plot indicates a

crossover as defined by two or more points within the search radius (see Section 3.5.2). Graphical inspection reveals that an adequate number of crossovers (i.e., greater than 1000) were detected to produce reliable statistics.

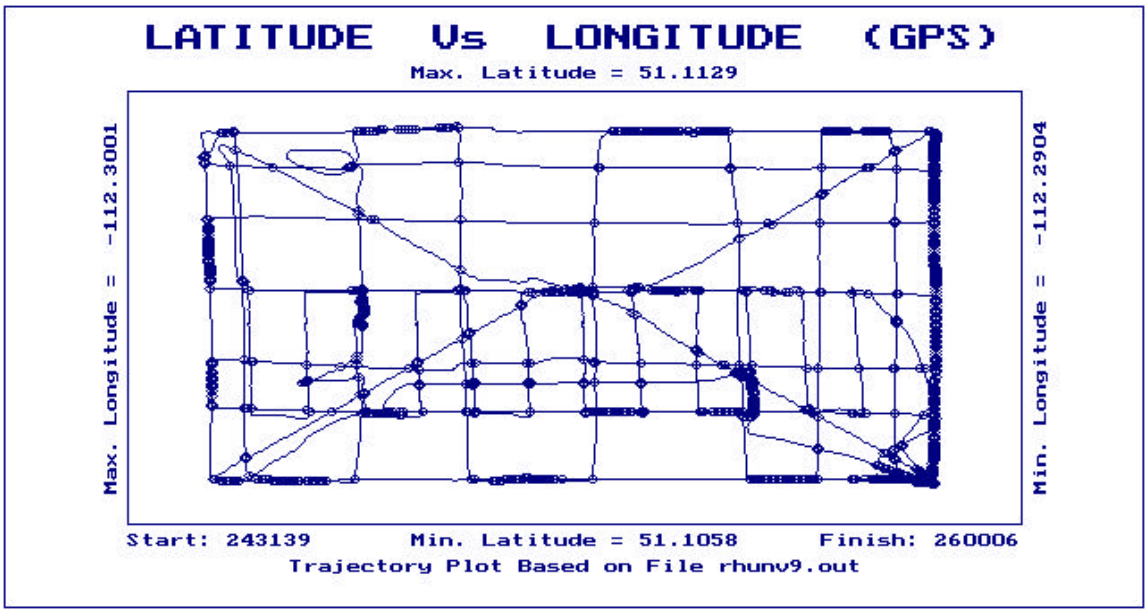

FIGURE 4.16 - Trajectory and Crossover Points (Nov. 9)

Figure 4.17 is the crossover distribution from the trajectory of November 9. A maximum difference of two metres occurred in the crossover detection. The RMS difference of 0.569 m in height is due to the sum of three different

sources; difference in geometry, true relief inside the search radius and position accuracy.

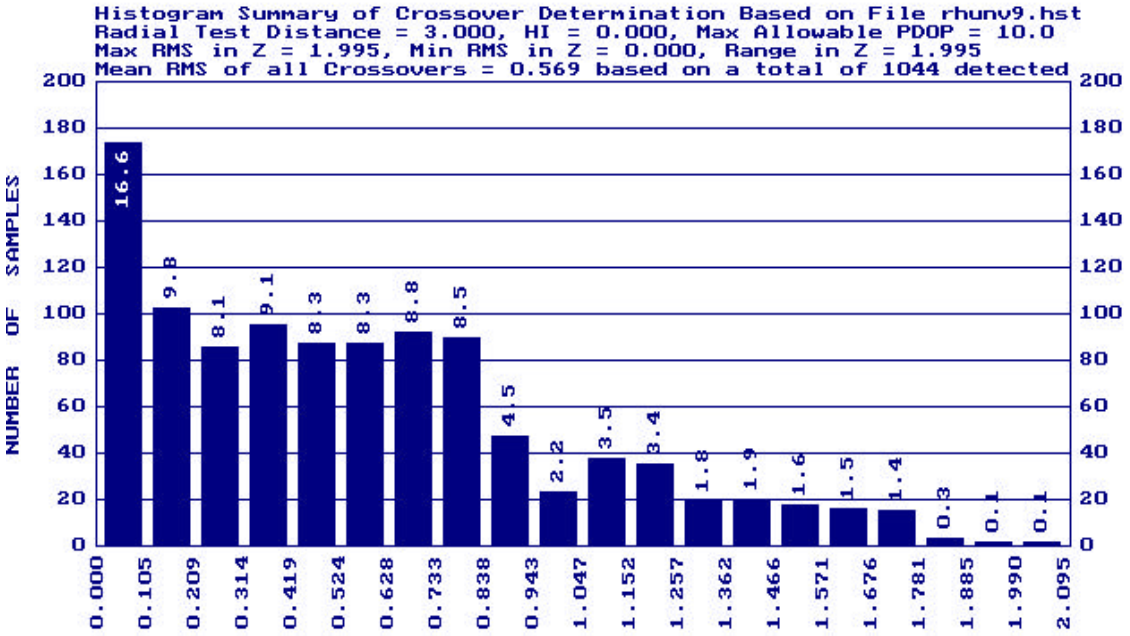

FIGURE 4.17 - Histogram of RMS Differences

To further examine the height repeatability during the same session, the same data set was re-run using the ***OTF*** phase solution. Results were much better due to the better position determination capability. The RMS of 0.108 m indicates that the predominate sources of error in the smoothed code solution are geometry, difference in measurement resolution and

multipath. If the relief variations within the search radius had been significant, the results of the two solutions would have been much closer in magnitude. The largest differences in height were confirmed to have occurred on a steep hillside where the relief is approximately 2 metres in a radius of 3 metres. One approach to removing the error due to true relief is to minimize the search radius. The result of this is fewer crossovers detected. The topography and vehicle dynamics should be considered when selecting a search radius.

The repeatability in height was also of interest for an inter-session comparison. Data sets that were six weeks apart were processed through ***X_OVER1*** to determine the effects of derived heights over time. A summary table of the RMS values for all tests performed for height repeatability is shown below. The trajectory plot shown in Figure 4.18 is the trajectory of November 9 superimposed over the two days (September 20, 21).

	November 9	September 20,21	Nov9, Sept20,21
Smoothed Code	0.569	0.250	0.432
OTF Phase	0.108	0.094	0.172

Table 4.4 - Crossover summary - Results in Metres

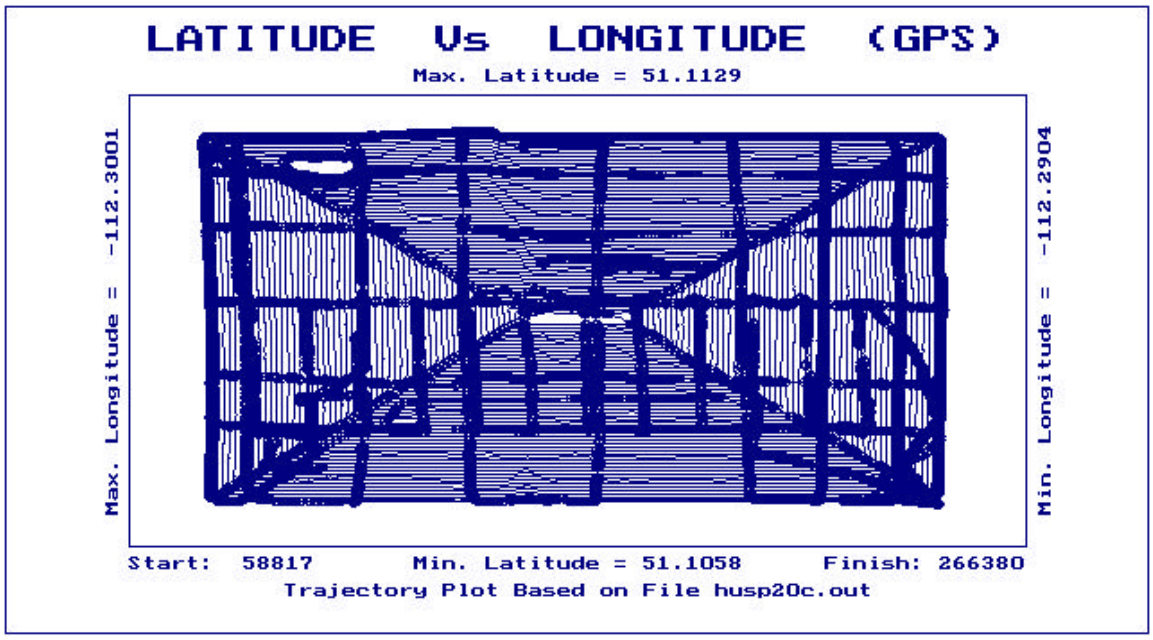

FIGURE 4.18 - Trajectories and Crossover Points (Nov. 9 and Sept. 20-21)

The results in table 4.4 verify that the DGPS heights derived are stable within the session and over time. The

accuracy required in height for this project is 1.0 m (RMS) and is delivered by both processing methods.

CHAPTER 5

RESULTS OF PHASE II AND REAL-TIME DGPS PERFORMANCE

Phase II is the implementation of the variable rate fertilizer application. Alberta Agriculture had specified the fertilizer blend and bands to be implemented for each field and laid out the grid pattern for navigation in the prescription map.

5.1 Field Test Regions

The design of each prescription map was determined by the field shape, ease of tillage or crop. Only sections of the fields where detailed soil samples had been taken were to undergo the variable rate and banding application. The remainder of the field would receive a blanket application as per the local farm operator. The results from the 1994 fall harvest will be layered over the spring 1994 fertilizer applications to study the crop response.

5.1.1 Bow Island

The Bow Island test region uses the west half of the irrigated section as shown in Figure 5.1. By selecting this portion of the field, the largest irrigated region would be in use and the pivot would not pose a field hazard. The soil samples were also performed in this region. Additionally, landscape specific soil samples were taken in and around the test region.

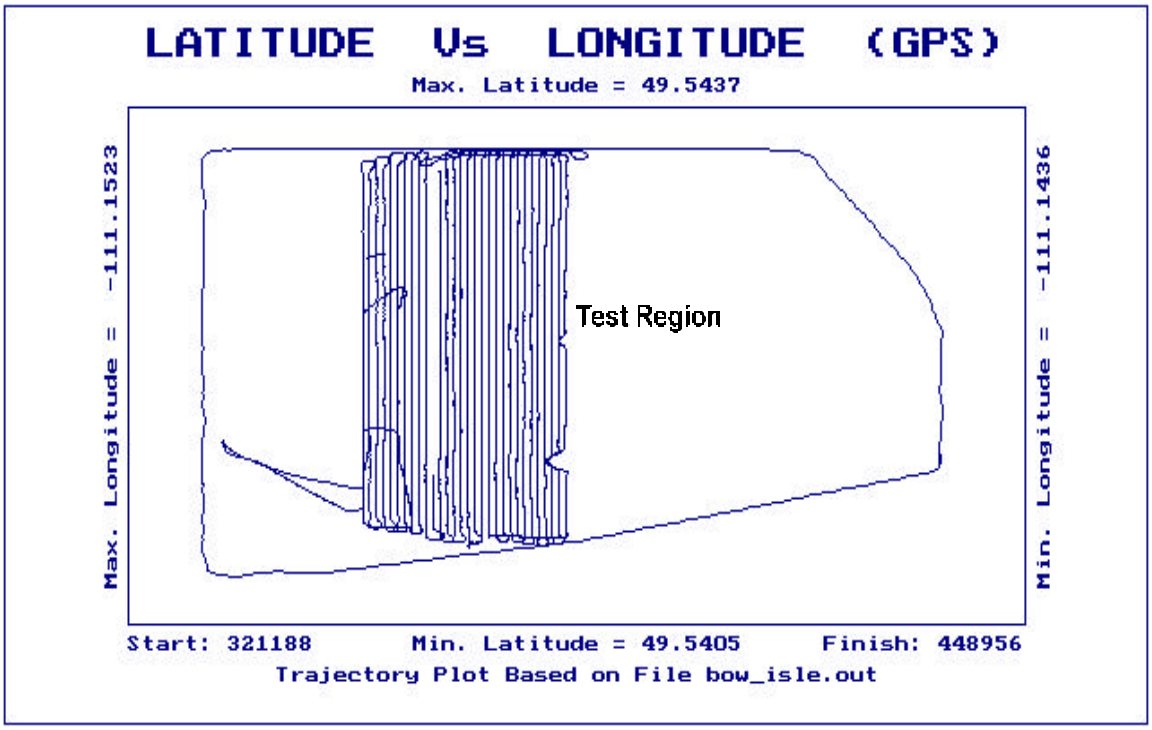

FIGURE 5.1 - Bow Island Test Region

5.1.2 Hussar

The Hussar test site was lateral in the east/west direction as this would allow long strips the length of the field and is compatible with the direction used in the remaining portion of the field at seeding and harvest time. Three sections as shown in Figure 5.2, were used to perform variable rate application as well as some strips for fixed banding. Extensive soil sampling had taken place throughout the field as well as landscape specific samples.

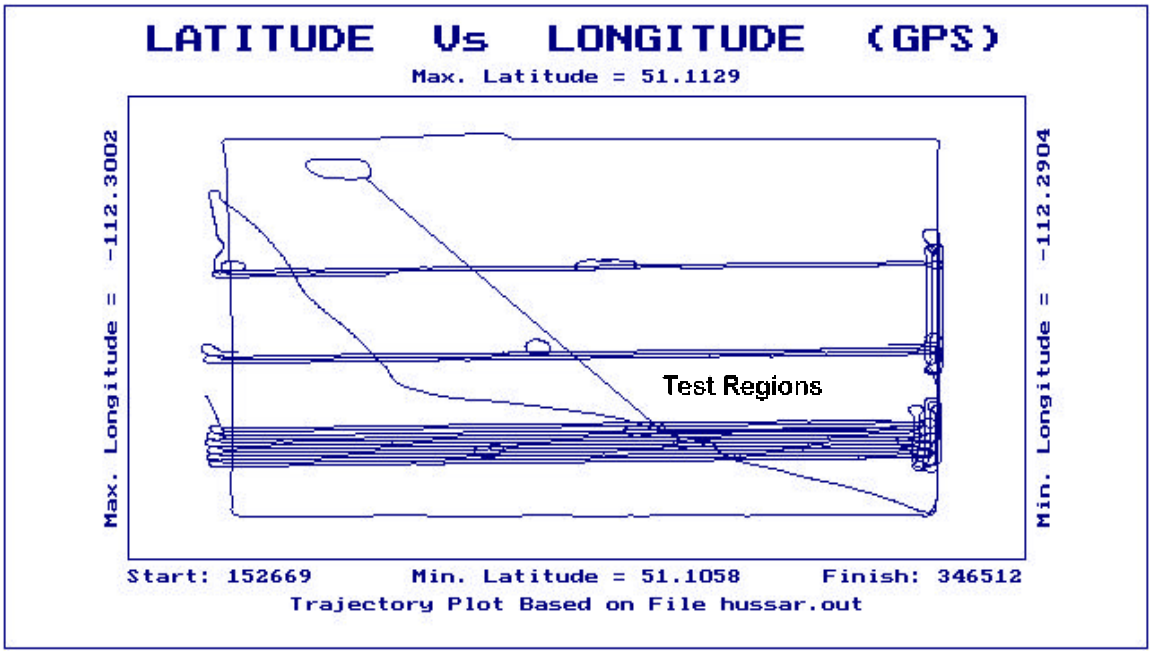

Figure 5.2 - Hussar Test Regions

5.1.3 Stettler

The Stettler site crop was to be put in a 315/135 degree azimuth referenced to geodetic north. This was due to the crop choice of canola. In order to protect the crop, the seed rows must be aligned with the local prevailing winds. The ***RTDGPS*** system was then used as a navigation system to place the tractor in the correct pattern as well as provide the necessary position determination for fertilizer blend and band weights. The test region is shown in Figure 5.3.

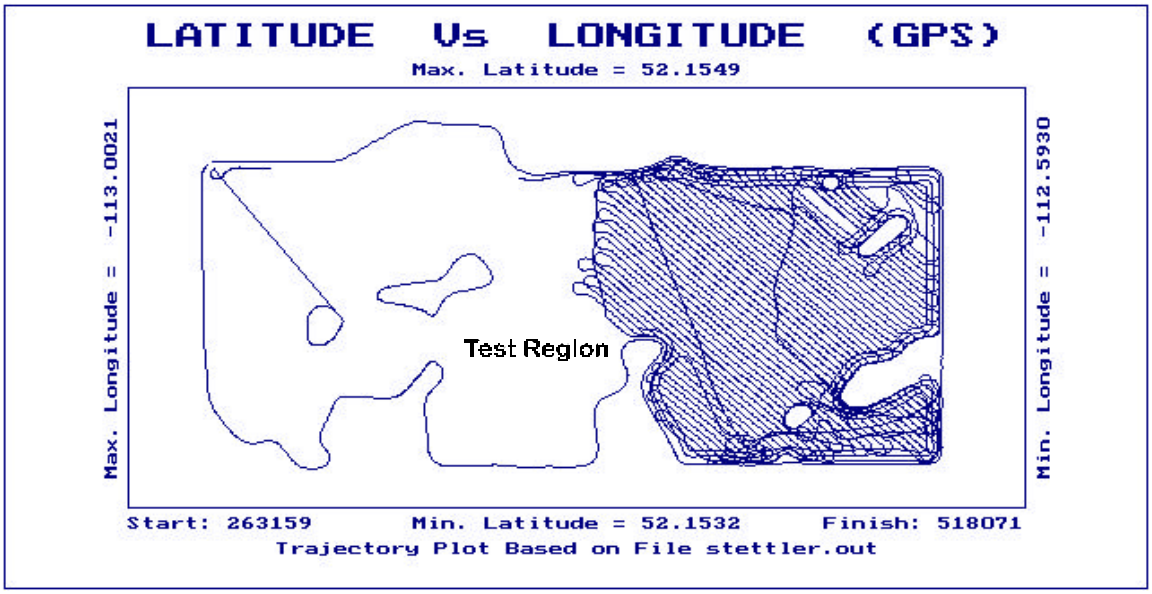

Figure 5.3 - Stettler Test Region

5.2 Real Time DGPS Performance

The performance analysis of the RT DGPS was evaluated in a similar manner as in Phase I. Using the ***OTF*** phase solution as a baseline, an epoch by epoch comparison was performed with the positions derived from the ***RTDGPS***. Some modifications were made to ***FLYVSC3N*** to allow for the removal of large position differences as seen in the line plots in Figures 5.5, 5.7 and 5.9. A rejection distance of two meters (spherical) was used at all sites. A running total of failed epochs (greater than

the rejection distance) was also kept to determine if the number of rejections was significant to the overall performance.

5.2.1 RT DGPS Vs OTF Phase Solution

The ***RTDGPS*** results at each site are compared to the ***OTF*** phase solution to evaluate the performance of the real time positioning system. Both the Bow Island and Stettler sites were completed in one day. The Hussar site was broken into two days to allow the Stettler site to be completed on schedule. It was returned to and completed the day after Stettler. Only the first day at Hussar is represented in the table 5.1 as day two was very short and non-continuous tracking problems created very few epoch comparisons because the ***OTF*** phase solution was not given sufficient continuous data to resolve the ambiguities.

Desc.	START	END	RMS	% Reject	Mean	# of Obs.
BI	**404950**	**448956**				**16935**
E			**0.158**	**1.81**	**-0.030**	
N			**0.192**	**1.84**	**0.051**	
H			**0.386**	**2.04**	**0.179**	

HU	**153840**	**167280**				**5738**
E			**0.210**	**1.48**	**0.070**	
N			**0.320**	**1.48**	**0.130**	
H			**0.520**	**3.12**	**0.170**	
ST	**263161**	**283756**				**14675**
E			**0.170**	**0.95**	**-0.060**	
N			**0.240**	**0.96**	**-0.020**	
H			**0.460**	**1.47**	**0.014**	

Table 5.1 - *RTDGPS* VS *OTF* Phase Position Comparison

The results expressed in table 5.1 indicate that a degradation in position accuracy was experienced in the transition from ***PMSC*** performance to ***RTDGPS*** performance. This is due primarily to the latency of the differential corrections in the presence of **SA**. Since the data rate was held fixed at 1 Hz, the effects of **SA** on the differential corrections were partly compensated for with the fast reaction of the linear prediction formula (Eqn 3.10). The residual effect of this prediction shows up in the position differences. Additionally, there is a difference in the remote station set ups for the real time portion. A chokering was used in Phase II to minimize multipath effects where no chokering was present in Phase I. Mean RMS values of 0.180 m,

0.250 m and 0.455 m in easting northing and height respectively reveal that the project accuracies have been maintained. The use of the chokering appears to have an insignificant effect on the overall position accuracy. The use of a chokering in Phase I may have produced slightly better results but is not necessary for the project requirements. Due to the constraints of antenna mounting, this is a great convenience.

5.2.2 *RTDGPS* Vs *SC* Post Mission

To quantify the absolute differences in the ***RTDGPS*** and post mission ***SC*** (PMSC) solution, an epoch by epoch comparison was also performed. The histograms of easting, northing and height differences confirm the degradation of the ***RTDGPS*** and a deficiency in the RT system is also apparent in the epoch by epoch line plots. The spikes are caused by an incomplete data string containing the differential corrections calculated at the monitor station. The string was not verified for completeness at the remote station resulting in spurious corrections being applied. This caused position spikes of up to 100 metres. The line plots in Figures 5.5, 5.7 and 5.9 have had the spikes removed.

The solution to the incomplete differential correction data string is to calculate the validity (i.e., checksum) of each string, append this value to the end of the string and transmit it to the remote station. Upon reception of the incoming data string, the checksum is re-calculated and compared to the transmitted value for integrity verification. If the string is rejected then the range correction applied is

computed from the linear prediction equation (Eqn. 3.10) using the most current range rate value.

To prevent the ***SC*** solution from degrading due to **SA** over successive epoch with no range corrections, a warning system was embedded into the ***RTDGPS*** software to issue a warning beep and status message when corrections were delayed longer than the data collection interval. Typically, the system was allowed to drift for 10 seconds using Eqn. 3.10. At this point, preliminary investigation showed that the **SC** accuracy had sufficiently degraded to the metre level and deteriorating quickly. The user is notified and the variable system shut off. The most common reason for loss of correction information was radio communications failures.

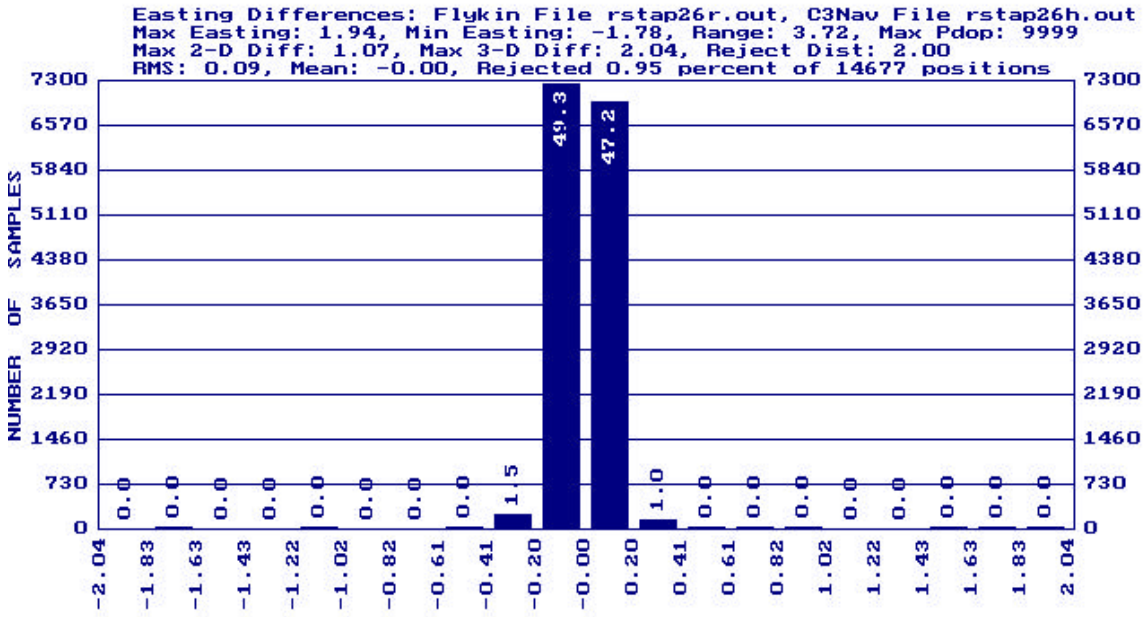

Figure 5.4 - Easting Differences (m) for *RTDGPS* Vs *PMSC*

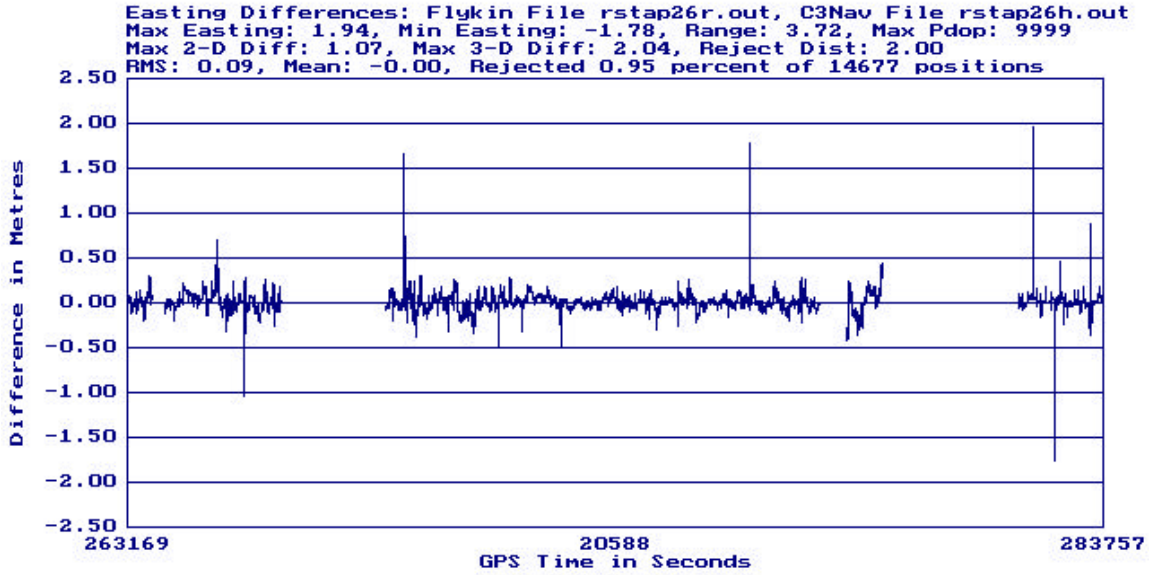

Figure 5.5 - Epoch by Epoch Comparison

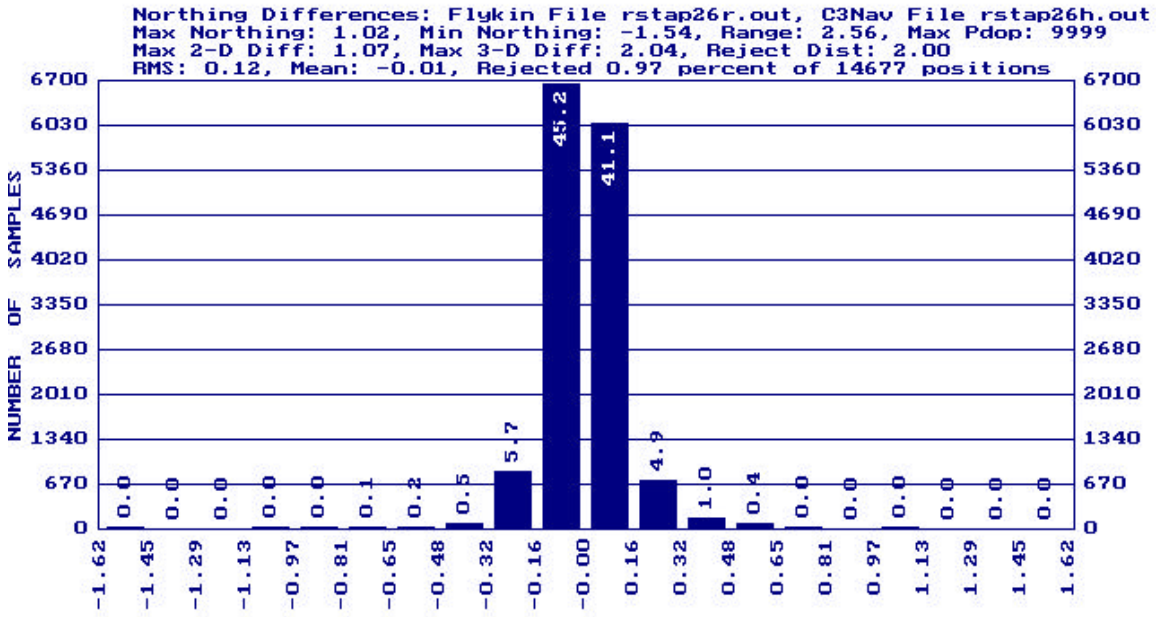

Figure 5.6 - Northing Differences (m) for *RTDGPS* Vs *PMSC*

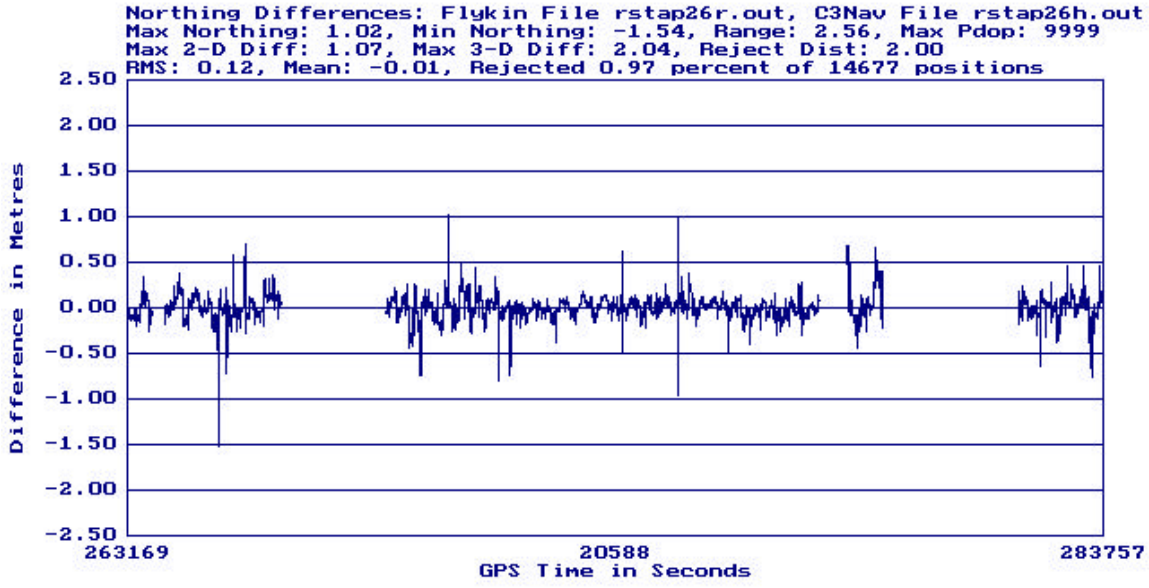

Figure 5.7 - Epoch by Epoch Comparison

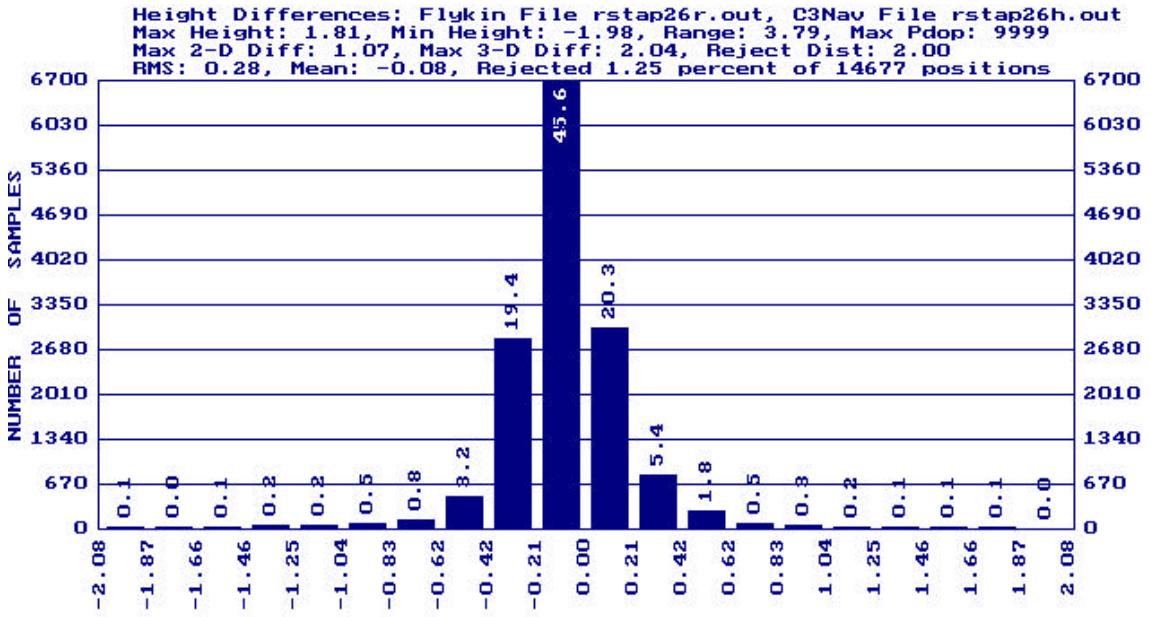

Figure 5.8 - Height Differences (m) for *RTDGPS* Vs *PMSC*

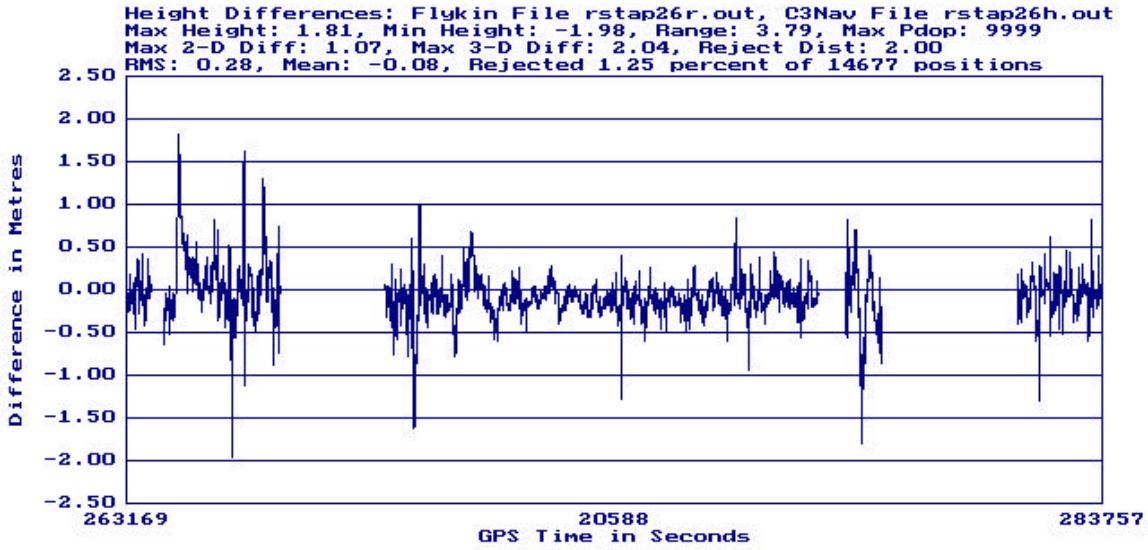

Figure 5.9 - Epoch By Epoch Comparison

The following table is a summary of the ***RT DGPS*** and the ***PMSC*** position comparison.

Desc.	START	END	RMS	% Reject	Mean	# of Obs.
BI	**403317**	**448956**				**21190**
E			**0.010**	**2.17**	**0.000**	
N			**0.120**	**2.46**	**0.000**	
H			**0.230**	**3.34**	**0.120**	
HU	**153840**	**167280**				**6309**
E			**0.110**	**1.51**	**0.030**	
N			**0.160**	**1.54**	**-0.030**	
H			**0.260**	**1.68**	**-0.140**	
ST	**263161**	**283756**				**14677**
E			**0.090**	**0.95**	**-0.005**	
N			**0.120**	**0.97**	**-0.010**	
H			**0.280**	**1.25**	**-0.083**	

Table 5.2 - *RTDGPS* VS *PMSC* Comparison - Results in metres

The amount of comparisons rejected were in the range of 1-2 percent are insignificant compared to the population size of the data. What is of concern is the resulting velocity computation. Since the determination of the velocity occurs in the position domain, the illustrated spikes in the above line plots will cause the velocity to spike in a similar manner. This was detected in the testing stages of the complete system from the screen which displayed the UTM easting and northing,

the current prescription map cell location as well as the velocity in metres per second. Since the origin of the spikes were unknown at the time, a safety valve was programmed into the communications to the MCU to reject any velocities that exceeded the airseeder’s rated maximum of 2.2 metres per second (five MPH). When a spurious velocity was detected, the servo motor speed was held constant at the previous value.

CHAPTER 6

CONCLUSIONS AND FUTURE RESEARCH

6.1 Thesis Conclusions

This thesis has outlined a precision farming approach in the Alberta agricultural community. The design and implementation of data collection via DGPS and DGPS integrated systems has been described and implemented through hardware and software. Crop variability has been measured and mapped at three site specific farming locations in Alberta.

Additional information such as soil variations, degree of salinity and topography have been collected, collated and draped over yield response via the GIS to assist in identifying the major causes and contributions each of crop response and future crop potential. From the previously mentioned information, agronomists have been able to identify regions that can be optimized via variable rate implementation of fertilizer blends and bands. The **DGPS** system and data capture procedures demonstrate that the spatial relationships

can be achieved with accuracies of 0.112 m , 0.194 m and 0.477 m in easting, northing and height respectively providing the reliability required for the farm site maps. The performance of the C/A code pseudorange used in differential mode was verified by a position comparison with the ***OTF*** phase solution technique.

A prescription map containing the proposed optimal input for each sub-field or a band for further crop reaction study was designed for each site. To carry out the prescription map instructions, a variable rate fertilizer applicator was integrated with a ***RTDGPS*** navigation and controller system that correlated the position in the field to the position on the prescription map. The real time system performance was slightly degraded (0.180 m , 0.250 m and 0.455 m in easting, northing and height respectively) compared to what was achieved in Phase I. The blend and band was extracted from the map, position and velocities determined and prescribed amounts of fertilizers placed into the field at the pre-defined location. The ***RTDGPS*** system performed adequately enough in comparison to post mission results to conclude that the prescription map requests were properly placed. The algorithms

for the ***RTDGPS*** software were adequate for the task but should be made more robust to accommodate the problems associated with ***SA,*** loss of radio communications and data integrity.

The use of a chokering on the farm vehicle in Phase II proved to be of little benefit based on the few centimetre degradation experienced in comparison to Phase I.

6.2 Future Research

Some improvements to the current prototype system are required. The addition of moisture sensors to the yield monitoring will assist in determining the relative variations in yield more accurately than assuming all crops have homogenous moisture content. Including information such as infrared and aerial photography will allow researchers to investigate other sources of non-optimal crop response.

Results from the previous and upcoming years will undoubtedly guide researchers in new directions for both hardware and software considerations as well as highlight field characteristics for closer investigation.

Improvements to the ***RTDGPS*** software to the stage of a full navigation system for additional farm use is the next logical step. Farm operations such as herbicide and pesticide applications or multi-tasking data collections system such as yield monitoring and weed infestation tracking will allow further optimization and control of land use.

Sustainable and economical farming is a growing concern among the agriculture community. The interest in precision farming is growing worldwide with an estimated 5% of the farms in the USA already using this type of technology. The economical benefit to the farming community can be a combination fertilizer saving and crop return of several dollars per acre (Goddard, 1994) to a high as $18.70 fertilizer savings per acre with no loss of crop yields (Mann, 1994).

As GPS receivers continue to become more affordable and computers more commonplace, the use of this technology will undoubtedly grow as the benefits are realized. Already in Europe there is legislation to prevent the overuse of farm

chemicals that cause environmental contamination (i.e. excess nitrogen leaching into the groundwater).

The Global Positioning System, computer advances and smart sensors are allowing farmers to perform the tasks that will allow farming to be more environmentally friendly, sustainable and economical for future generations.

REFERENCES

Anderson, N. (1994) “Field Navigation System” Patent application, Concord, Fargo North Dakota.

Bentham, Murray J. (1994) “Parkland Agriculture Research Initiative (PARI) Decision Support System (DSS)/Expert Systems(ES).” 16th Annual Meeting of the Alberta Conservation and Tillage Society.

Blachut, T.J., A. Chrzanowski and J.H. Saastamoinen (1979) “Urban Surveying and Mapping”, Springer-Verlag New York Inc. Printed in the United States of America.

Cannon, M.E. and G. Lachapelle (1992) “C3Nav Operating Manual.” Department of Geomatics Engineering, University of Calgary, Calgary, Alberta. Version 1.3

Cannon, M.E. and G. Lachapelle (1992a) “Analysis of High Performance C/A Code GPS Receiver in Kinematic Mode.” Navigation, Vol. 39, N0. 3, The Institute of Navigation, Alexandria, VA, pp. 285-289.

Evans, A. G. (1986) “Comparison of GPS Pseudorange and Biased Doppler Range Measurements to Demonstrate Signal Mulipath Effects.” Proceedings of the Fourth International Geodetic Symposium on Satellite Positioning, Austin, Texas, April 28 - May 2, Vol. 1: pp. 573-587.

Falkenberg, W., T. Ford, J. Neuman, P. Fenton, M.E. Cannon and G. Lachapelle (1992) “Precise Real-Time Kinematic Differential GPS Using a Cellular Radio Modem.” Presented at the IEEE Position, Location and Navigation Symposium, PLANS 92, Monterey, Ca. March 24-27, 1994.

Fenton, P., W. Falkenberg, T. Ford, K.Ng, and A. J. Van Dierendonk, (1991) “NovAtel’s GPS Receiver, the High Performance OEM Sensor of the Future.” Proceedings of GPS91, Institute of Navigation, Alexandria, VA., pp.49-58.

Geonics Limited (1980), J. D. McNeil, “Electrical Conductivity of Soil and Rocks.” Technical Note-21.

Goddard, T. W. (1994) “Consequences of Ignoring Variability” 6th Annual Breton Plots Field Day, June 30,1994.

GRE America Inc. (1993) “GINA - Global Integrated Network Access.” Users Manual, Revision 2.

Hofmann-WellenHof, B, H. Lichtenegger and J. Collins (1992) “GPS Theory and Practice” Second Edition, Springer-Verlag Wien New York.

Krakiwsky, E.J. and P. Gagnon (1987) “Papers For The CISM Adjustment and Analysis Seminars”, The Canadian Institute of Surveying and Mapping, January, 1987, pp. 108-149.

Lachapelle, G., M.E. Cannon, B. Townsend and R. C. McKenzie (1992) “Mapping Soil Salinity with Satellite-Based positioning Methods.” Presented at the 38th Meeting of the Canadian Soil Science, Edmonton, Alberta, 9-13 August, 1992.

Lachapelle, G., M. E. Cannon, G. Lu, (1992a) “High Precision Navigation With Emphasis on Carrier Phase Ambiguity Resolution.” Submitted to Marine Geodesy, Vol. 15, pp. 253-269.

Lachapelle, G., C. Liu, G. Lu, B. Townsend, M. E. Cannon and R. Hare (1993) "Precise Marine DGPS Positioning Using P Code and High Performance C/A Code Technologies." Proceedings of the National Technical Meeting, The Institute of Navigation, Alexandria, VA, pp. 241-250.

Martin, E. H. (1980) "GPS User Equipment Models." Navigation, The Institute of Navigation, Vol. 1, pp. 109-118.

MANN, John (1994) "GPS Down on the Farm." GPS World - Washington View, September 1994, pp. 18.

McKenzie, R. C., W. Chomistek and N. F. Clark (1989) "Conversion of Electromagnetic Induction Readings to Saturated Paste Extract Values in Soils for Different Temperature, Texture and Moisture Conditions." Canadian Journal of Science 69: pp. 25-32, February, 1989.

Motorola Inc. (1991) "M68HC11EVB Evaluation Board" Reference Manual.

Myers, A. (1993) “AG Leader Yield Monitor 2000.” Users manual and installation guide. AG Leader Technologies Inc.

Nyborg, M. (1994) “Tillage, straw disposal and Fertilizer nitrogen: the Influence on yield of Continuous Barley and on Soil Organic Content at Breton.” 6th Annual Breton Plots Field Day, June 30,1994.

Rhoades, J. D. and D. L. Corwin (1981) “Determining Soil Electrical Conductivity-Depth Relations Using an Inductive Electromagnetic Soil Conductivity Meter.” Soil Science Society Am. Journal 43, pp. 255-260.

Robertson, J. A. and K. W. Domier (1994) “Placements and Residual Effects of P Fertilizer.” 6th Annual Breton Plots Field Day, June 30,1994.

Scheuller, John K. (1992) “A Review and Integrating Analysis of Spatially-Variable Control of Crop Production.” Fertilizer Research 33: 1-34, 1992, Kluwer Academic Publishers.

Tiemeyer, B., M.E. Cannon, G. Lu and G. Schanzer (1994) "Ambiguity Resolution of L1 GPS Carrier Wave Measurements for High Precision Aircraft Navigation." Submitted for Presentation at National Technical Meeting of The Institute of Navigation, San Diego, 24-26 January, 1994.

Van Dierendonk A. J., P. Fenton, T. Ford (1992) "Theory and Performance of Narrow Correlator Spacing in a GPS Receiver." Navigation: Journal of the Institute of Navigation, Vol. 39, No. 3, Fall 1992, Printed in U.S.A.

Wells, D. E., N. Beck, D. Delikaraoglou, A. Kleusberg, E.J. Krakiwsky, G. Lachapelle, R. B. Langley, M. Nakiboglu, K. P. Schwarz, J. M. Tranquilla, P. Vanicek, (1987) "Guide to GPS Positioning" Canadian GPS Associates, Fredericton New Brunswick, Canada.

Wollenbuapt, N. C., J. L. Richardson, J. E. Ross and E. C. Doll (1986) "A Rapid Method for Estimating Weighted Soil Salinity from Apparent Electrical Conductivity Measured with an Above Ground Electromagnetic

Induction Meter.” Canadian Journal of Soil Science: 66, pp. 315-321.